

# 1 Supplementary material for LHCb-PAPER-2022-039

## 1.1 Nominal fit

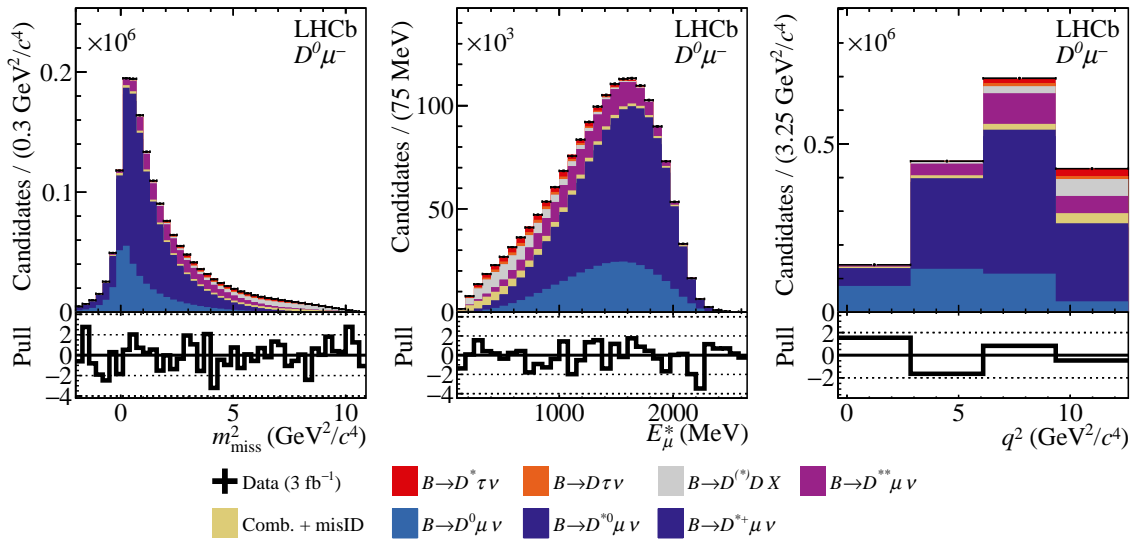


Figure 1: Distributions of (left) missing mass squared, (middle) lepton energy, and (right)  $q^2$ , overlaid with the projections of the fit model in the  $D^0 \mu^-$  signal region.

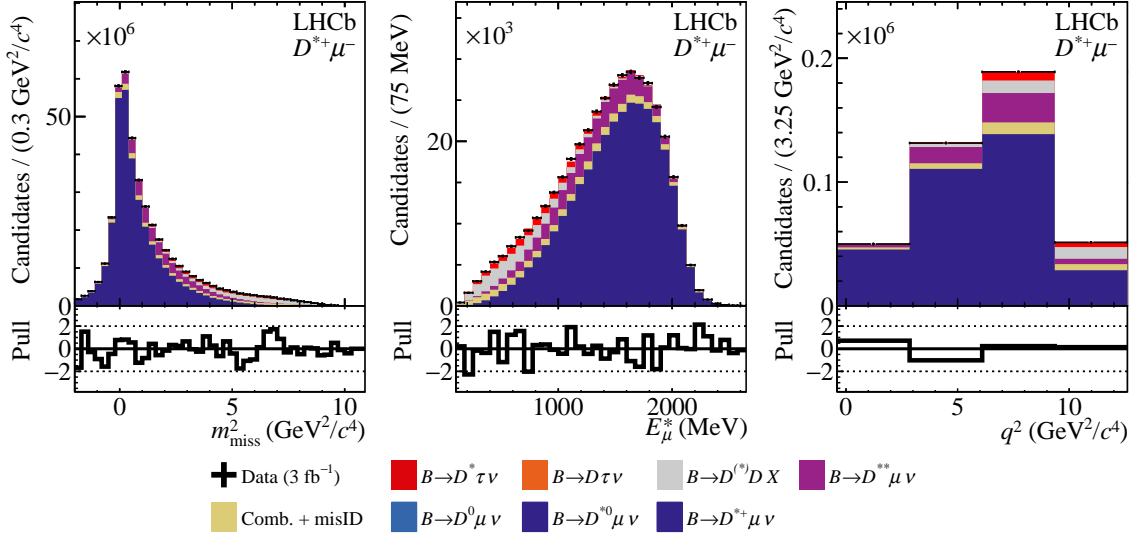


Figure 2: Distributions of (left) missing mass squared, (middle) lepton energy, and (right)  $q^2$ , overlaid with the projections of the fit model in the  $D^{*+}\mu^-$  signal region.

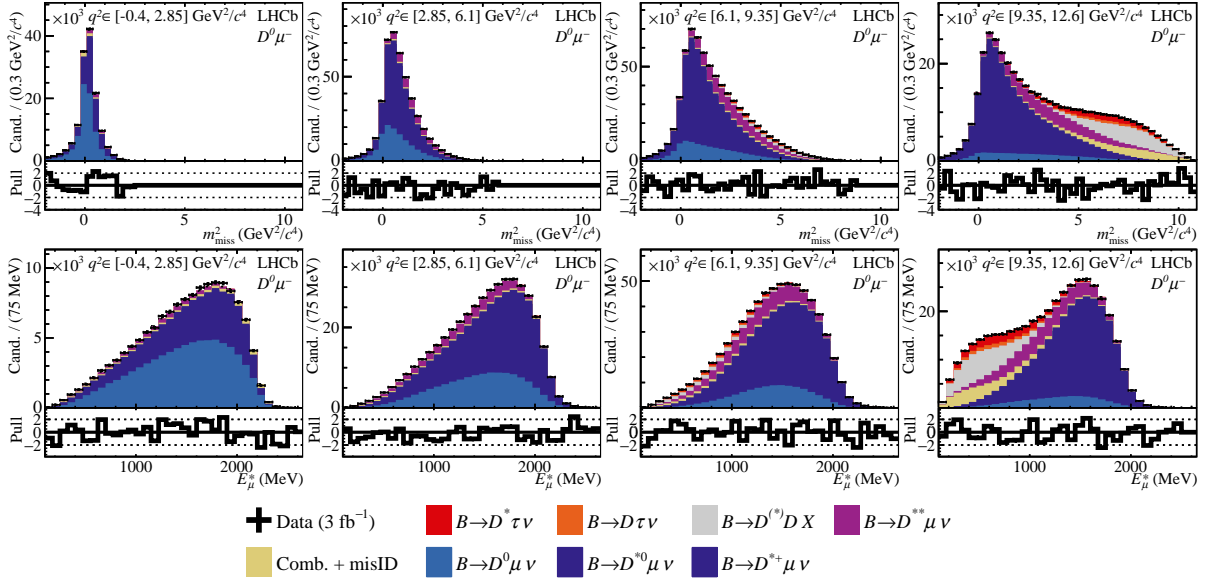


Figure 3: Distributions of (top row) missing mass squared and (bottom row) lepton energy overlaid with the projections of the fit model in the  $D^0\mu^-$  signal region, in the four bins of  $q^2$ .

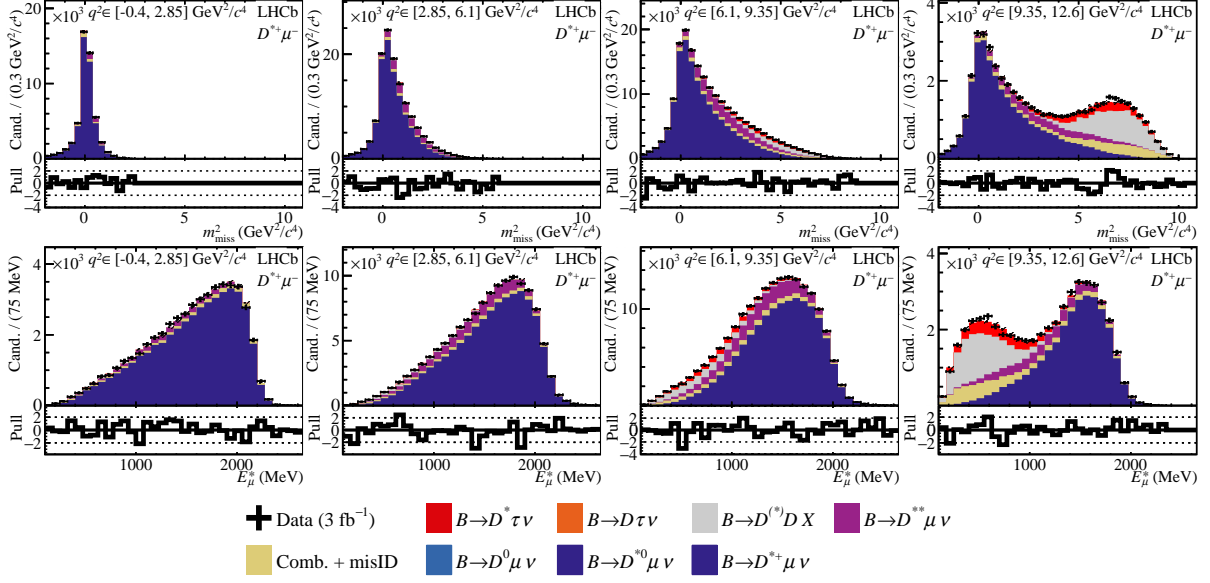


Figure 4: Distributions of (top row) missing mass squared and (bottom row) lepton energy overlaid with the projections of the fit model in the  $D^{*+}\mu^-$  signal region, in the four bins of  $q^2$ .

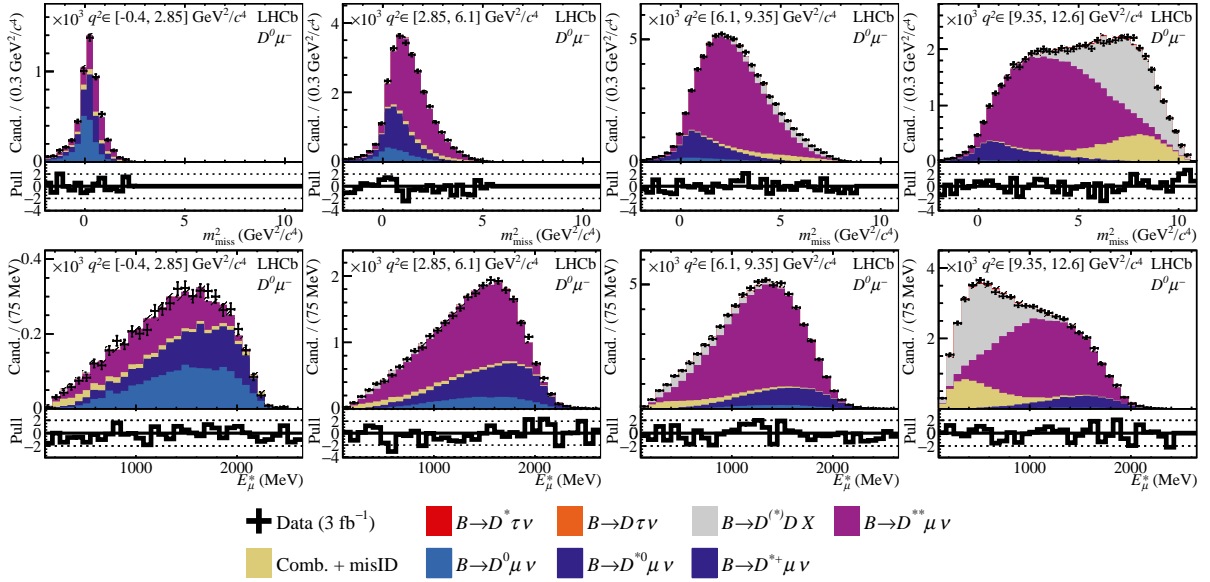


Figure 5: Distributions of (top row) missing mass squared and (bottom row) lepton energy overlaid with the projections of the fit model in the  $D^0\mu^-$  with exactly one extra pion consistent with the  $B$  vertex, in the four bins of  $q^2$ .

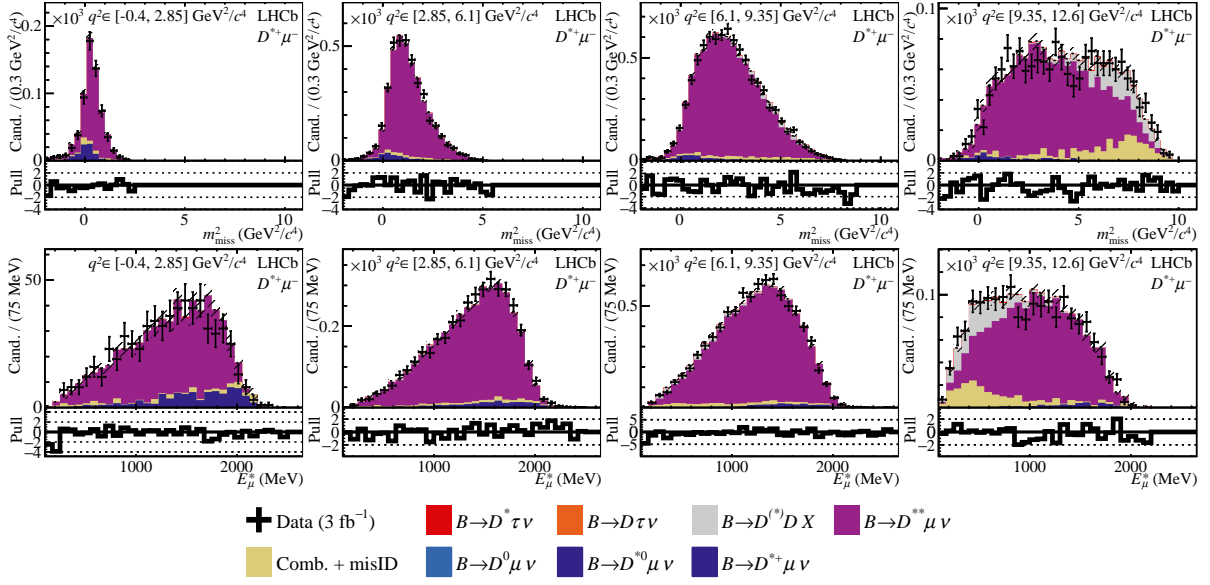


Figure 6: Distributions of (top row) missing mass squared and (bottom row) lepton energy overlaid with the projections of the fit model in the  $D^{*+}\mu^-$  with exactly one extra pion consistent with the  $B$  vertex, in the four bins of  $q^2$ .

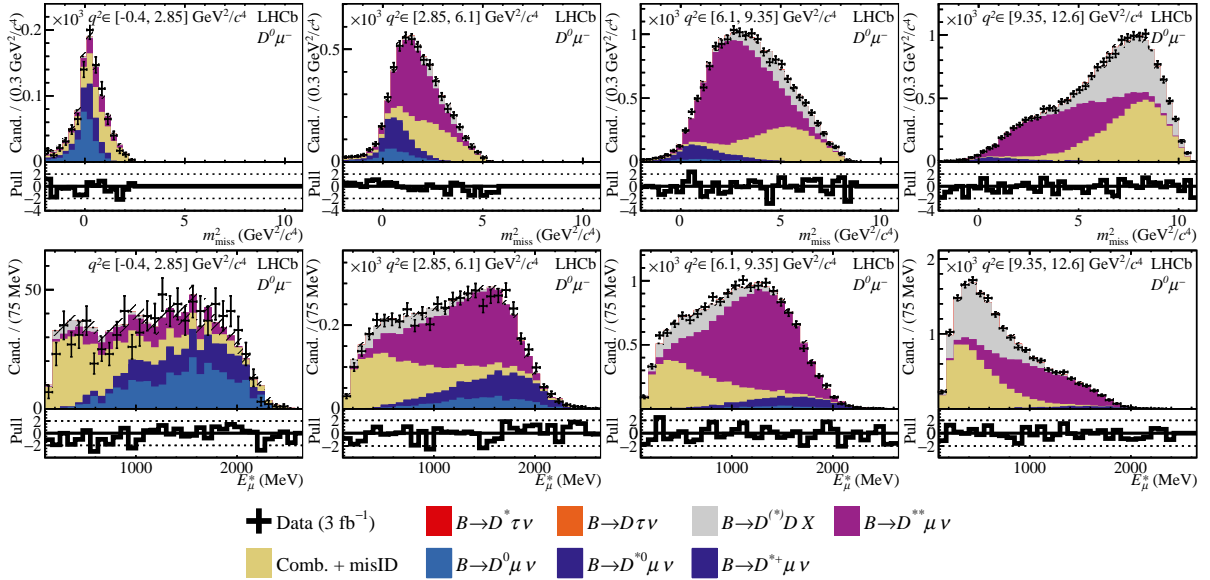


Figure 7: Distributions of (top row) missing mass squared and (bottom row) lepton energy overlaid with the projections of the fit model in the  $D^0\mu^-$  region with exactly two extra opposite-sign pions consistent with the  $B$  vertex, in the four bins of  $q^2$ .

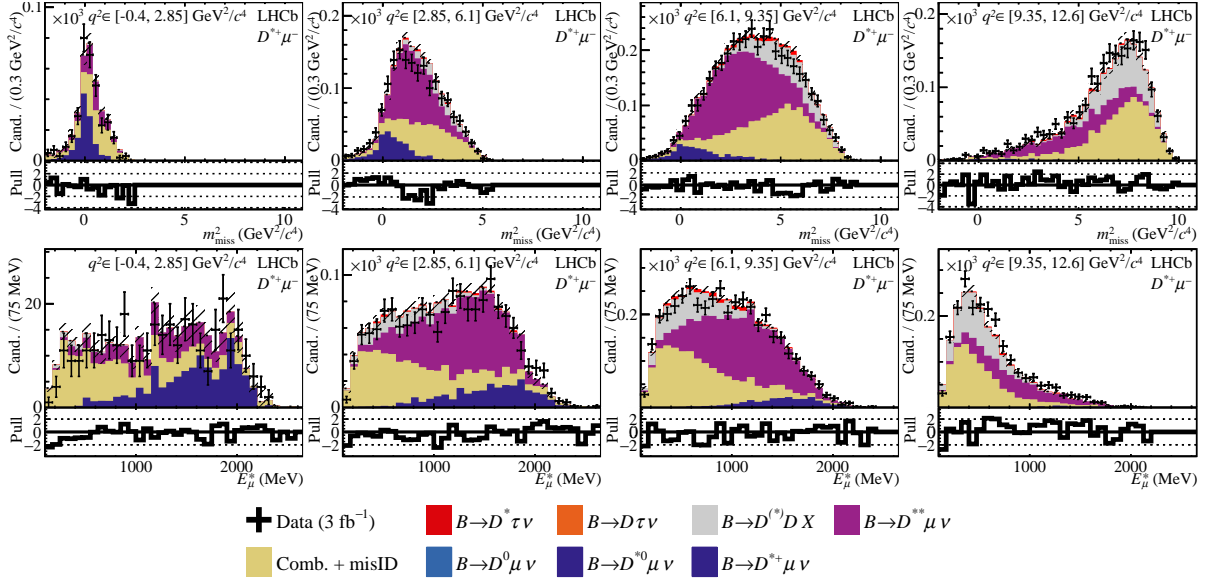


Figure 8: Distributions of (top row) missing mass squared and (bottom row) lepton energy overlaid with the projections of the fit model in the  $D^{*+}\mu^-$  region with exactly two extra opposite-sign pions consistent with the  $B$  vertex, in the four bins of  $q^2$ .

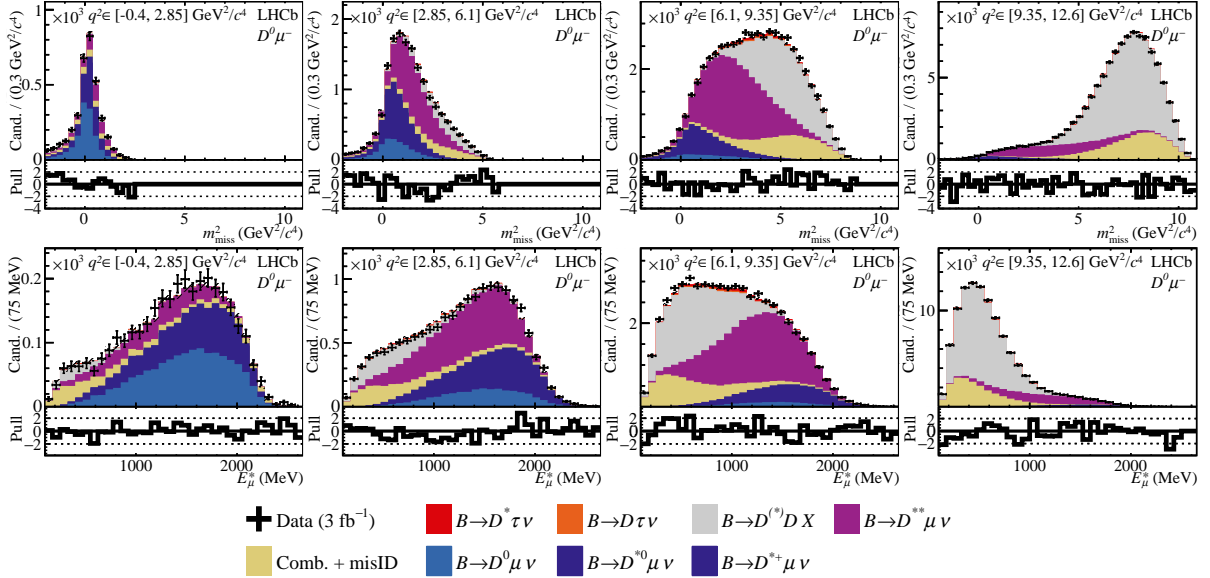


Figure 9: Distributions of (top row) missing mass squared and (bottom row) lepton energy overlaid with the projections of the fit model in the  $D^0\mu^-$  region with at least one kaon of either sign and no restrictions on the number of additional tracks consistent with the  $B$  vertex, in the four bins of  $q^2$ .

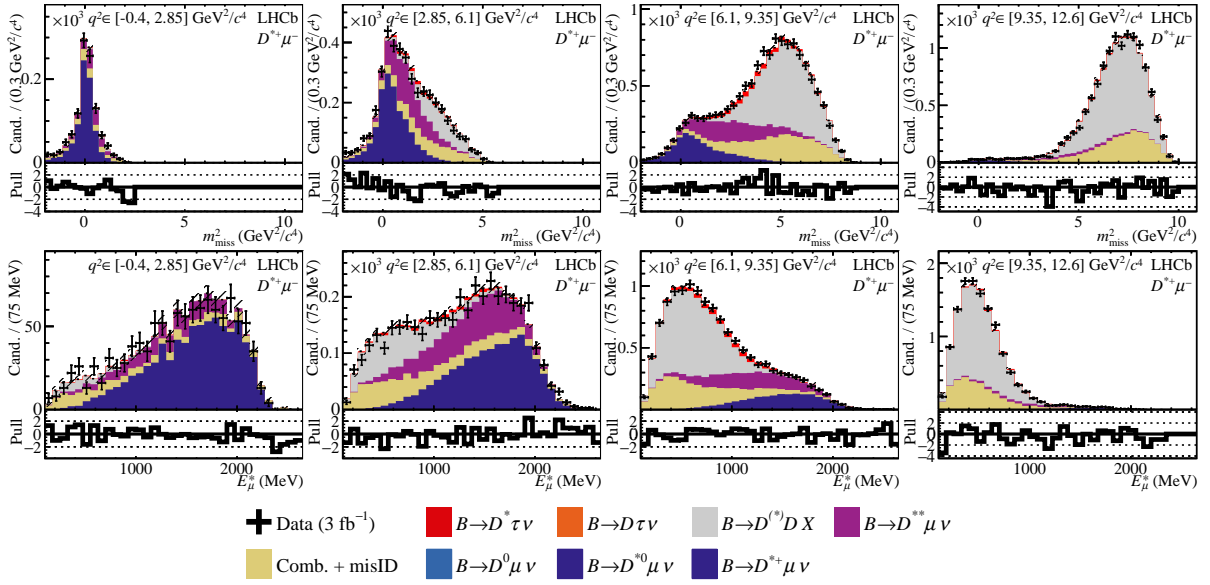


Figure 10: Distributions of (top row) missing mass squared and (bottom row) lepton energy overlaid with the projections of the fit model in the  $D^{*+} \mu^-$  region with at least one kaon of either sign and no restrictions on the number of additional tracks consistent with the  $B$  vertex, in the four bins of  $q^2$ .

## 1.2 Additional fit validation regions

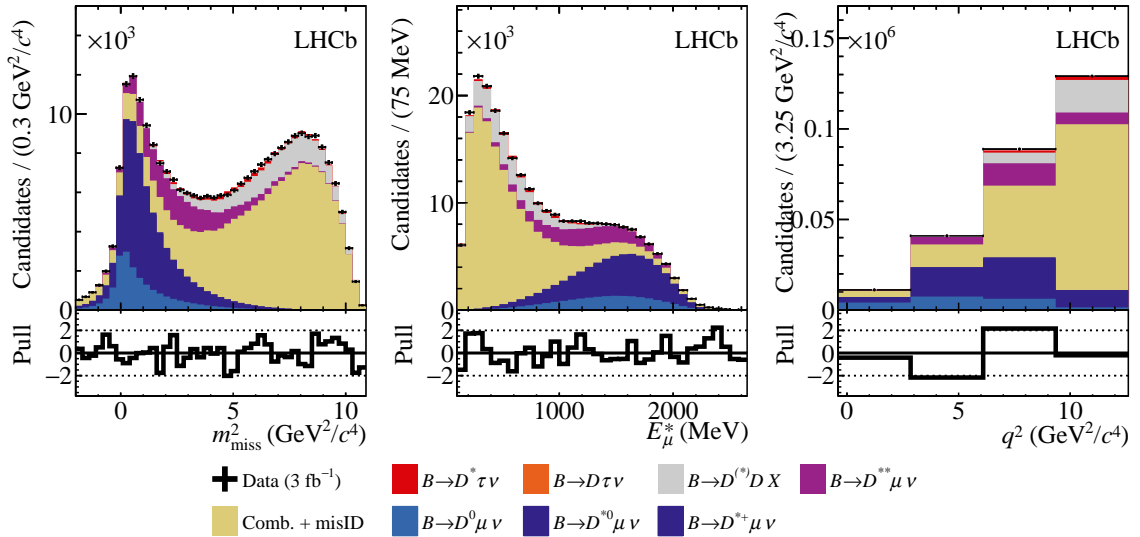


Figure 11: Distributions of (left) missing mass squared, (middle) lepton energy, and (right)  $q^2$ , overlaid with the projections of the fit model in the  $D^0 \mu^-$  region which fails the custom muon ID requirement.

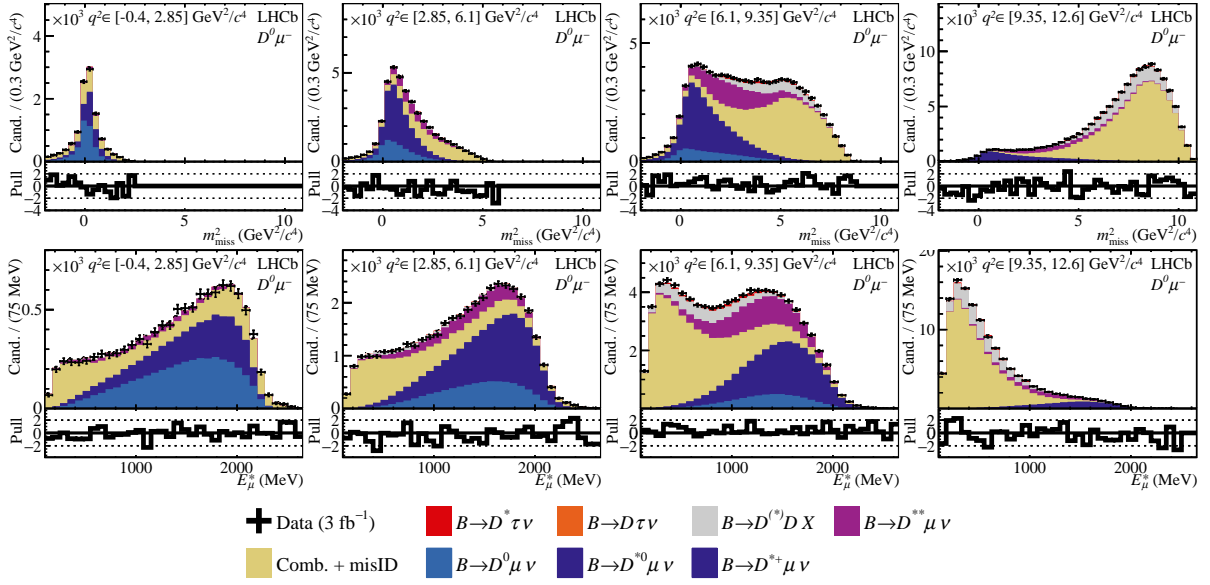


Figure 12: Distributions of (top row) missing mass squared and (bottom row) lepton energy overlaid with the projections of the fit model in the  $D^0\mu^-$  region which fails the custom muon ID requirement, in the four bins of  $q^2$ .

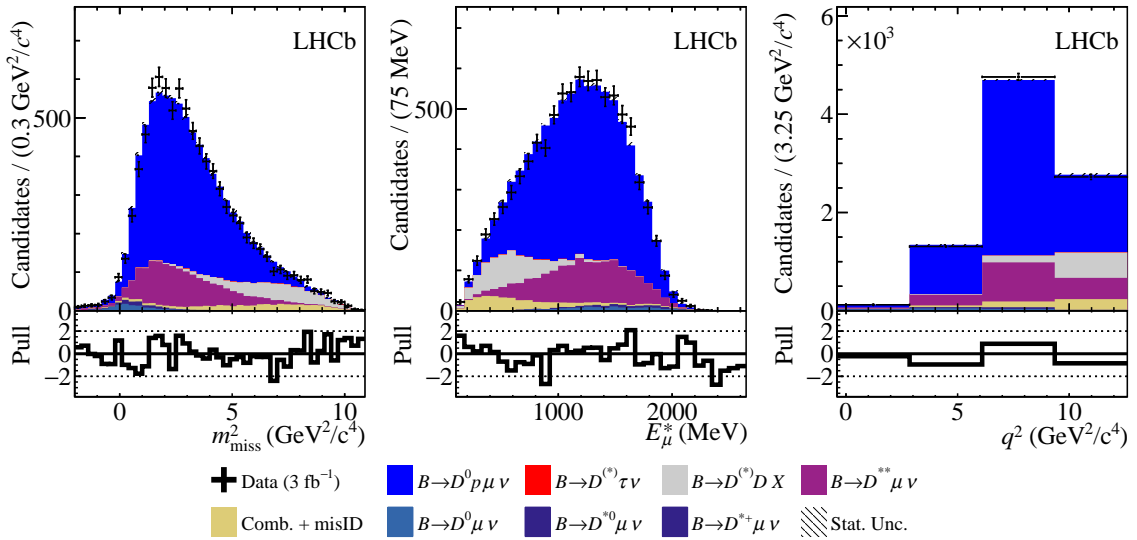


Figure 13: Distributions of (left) missing mass squared, (middle) lepton energy, and (right)  $q^2$ , overlaid with the projections of the fit model in the  $D^0\mu^-$  region with exactly one proton consistent with the  $B$  vertex. This fit includes the duplicated  $D^{**}$  components, collectively labelled as  $B \rightarrow D^0 p \mu \nu$ . The label stat. unc. refers to the statistical uncertainty on the fitted sum of templates.



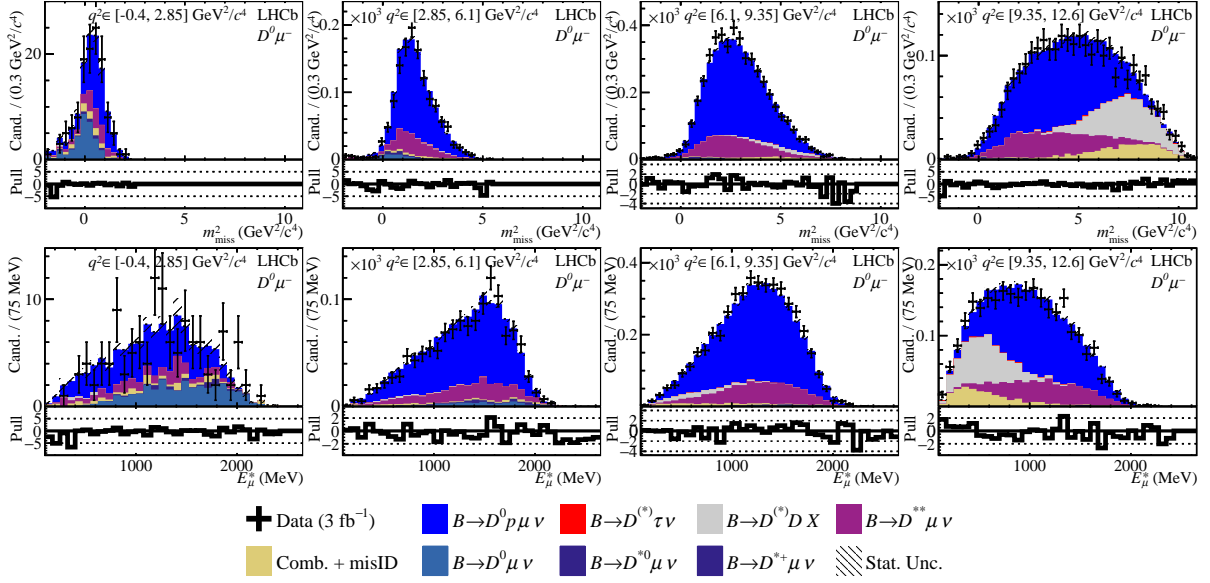


Figure 14: Distributions of (top row) missing mass squared and (bottom row) lepton energy overlaid with the projections of the fit model in the  $D^0\mu^-$  region with exactly one proton consistent with the  $B$  vertex, in the four bins of  $q^2$ . This fit includes the duplicated  $D^{**}$  components, collectively labelled as  $B \rightarrow D^0 p \mu \nu$ . The label “stat. unc.” refers to the statistical uncertainty on the fitted sum of templates.

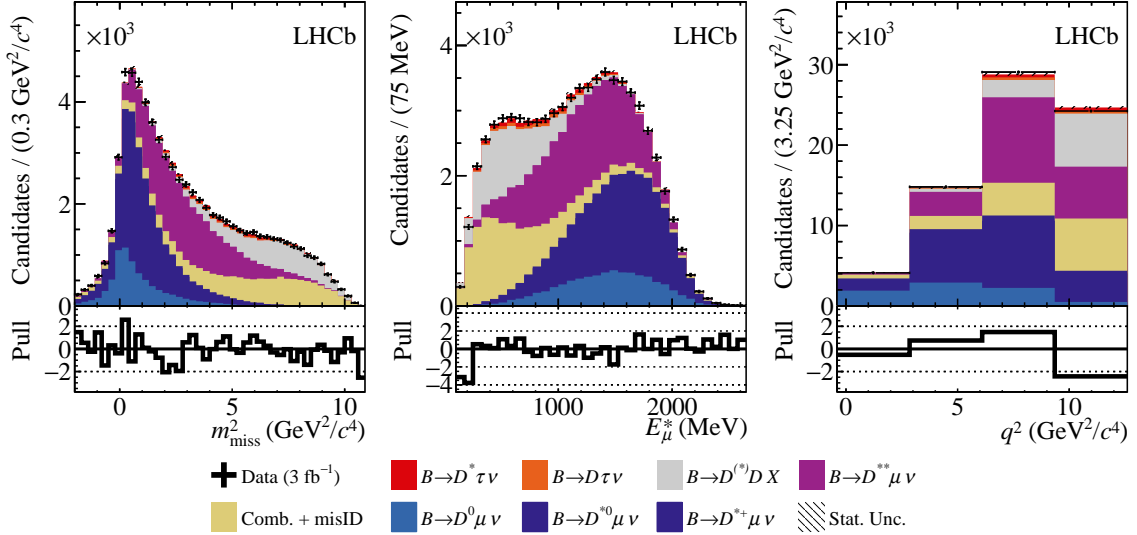


Figure 15: Distributions of (left) missing mass squared, (middle) lepton energy, and (right)  $q^2$ , overlaid with the projections of the fit model in the  $D^0\mu^-$  region with one extra pion with identical charge to the muon consistent with the  $B$  vertex. The label “stat. unc.” refers to the statistical uncertainty on the fitted sum of templates.

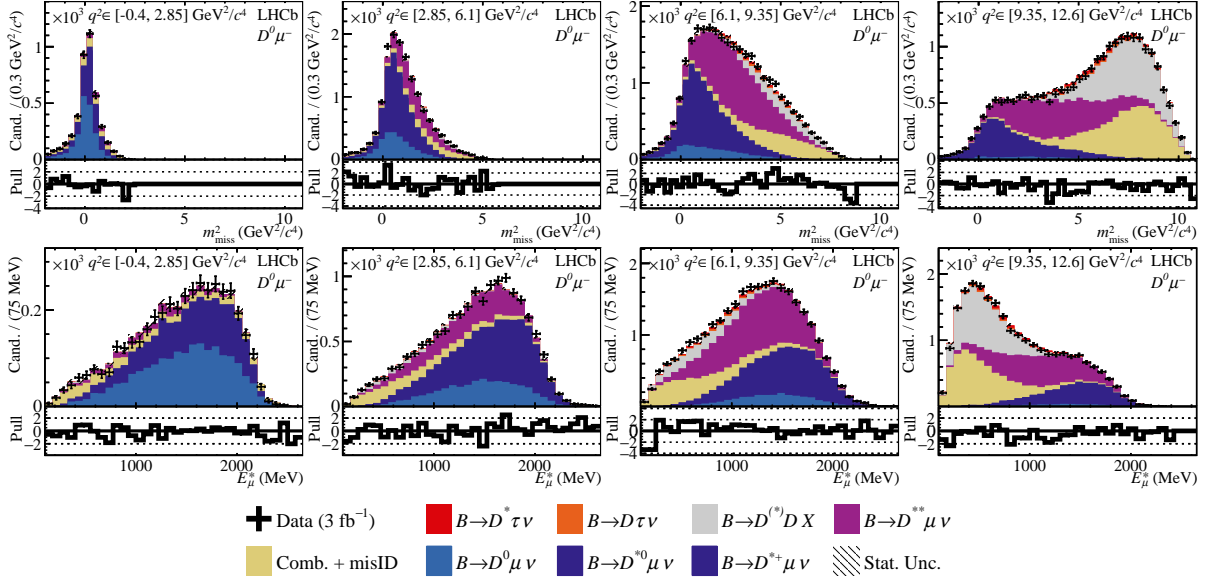


Figure 16: Distributions of (top row) missing mass squared and (bottom row) lepton energy overlaid with the projections of the fit model in the  $D^0\mu^-$  region with one extra pion with identical charge to the muon consistent with the  $B$  vertex, in the four bins of  $q^2$ . The label “stat. unc.” refers to the statistical uncertainty on the fitted sum of templates.

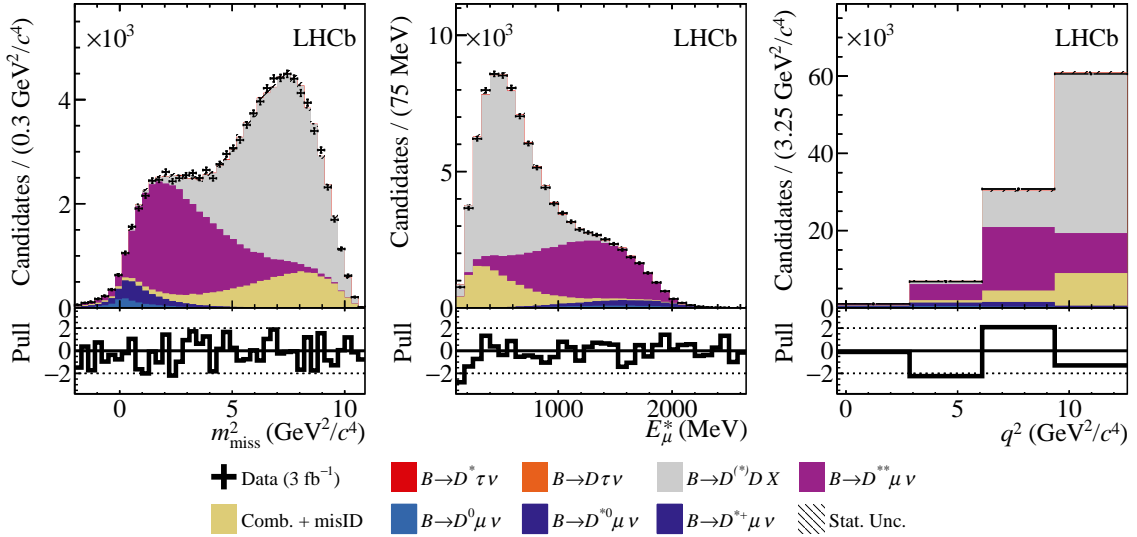


Figure 17: Distributions of (left) missing mass squared, (middle) lepton energy, and (right)  $q^2$ , overlaid with the projections of the fit model in the  $D^0\mu^-$  region with at least one kaon of opposite charge to the muon, and no restrictions on the number of additional tracks consistent with the  $B$  vertex. The label “stat. unc.” refers to the statistical uncertainty on the fitted sum of templates.

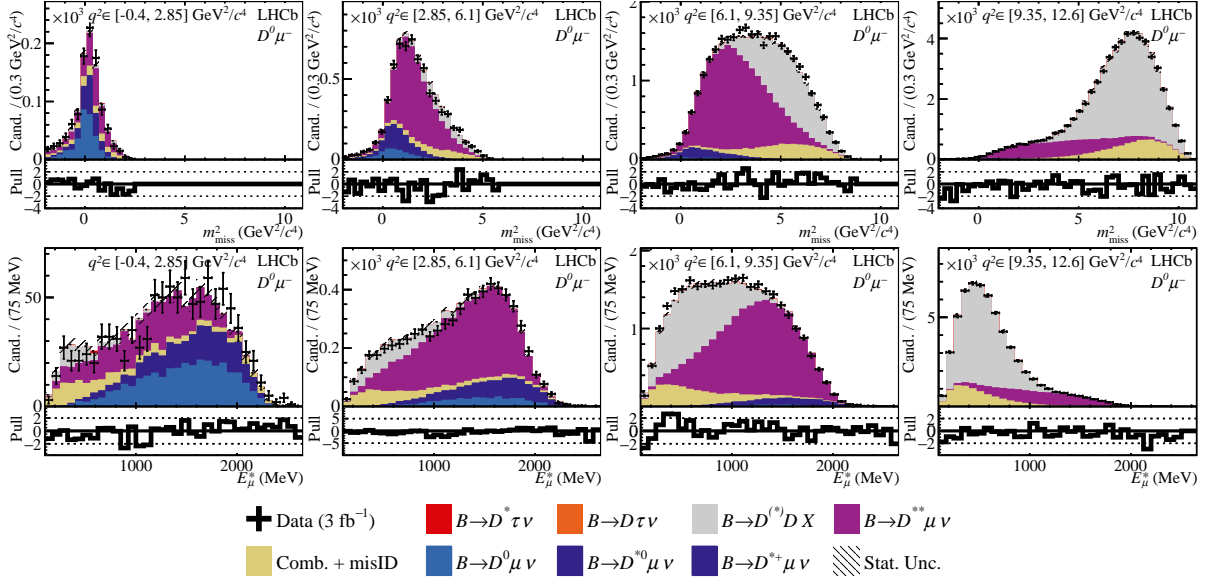


Figure 18: Distributions of (top row) missing mass squared and (bottom row) lepton energy overlaid with the projections of the fit model in the  $D^0\mu^-$  region with at least one kaon of opposite charge to the muon, and no restrictions on the number of additional tracks consistent with the  $B$  vertex, in the four bins of  $q^2$ . The label “stat. unc.” refers to the statistical uncertainty on the fitted sum of templates.

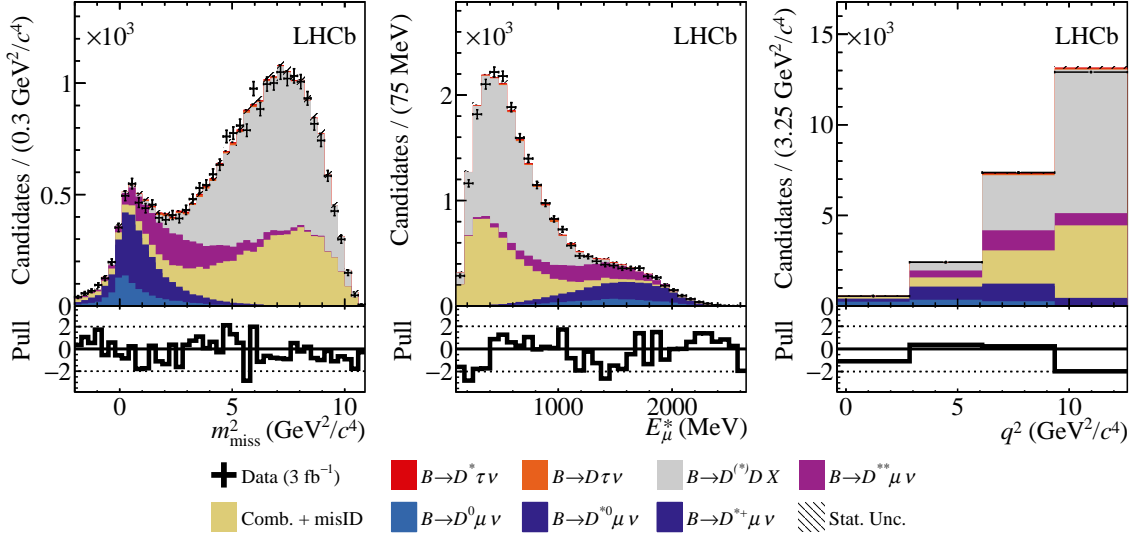


Figure 19: Distributions of (left) missing mass squared, (middle) lepton energy, and (right)  $q^2$ , overlaid with the projections of the fit model in the  $D^0\mu^-$  region with at least one kaon of identical charge to the muon, and no restrictions on the number of additional tracks consistent with the  $B$  vertex “DD\_WSK” category.

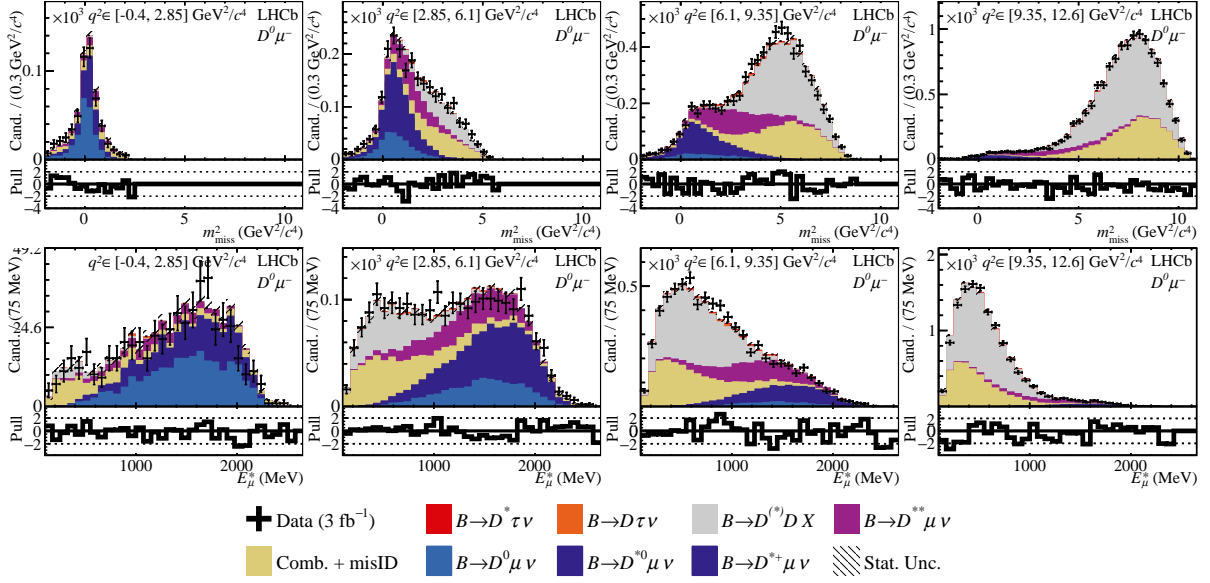


Figure 20: Distributions of (top row) missing mass squared and (bottom row) lepton energy overlaid with the projections of the fit model in the  $D^0\mu^-$  region with at least one kaon of identical charge to the muon, and no restrictions on the number of additional tracks consistent with the  $B$  vertex, in the four bins of  $q^2$ . The label “stat. unc.” refers to the statistical uncertainty on the fitted sum of templates.

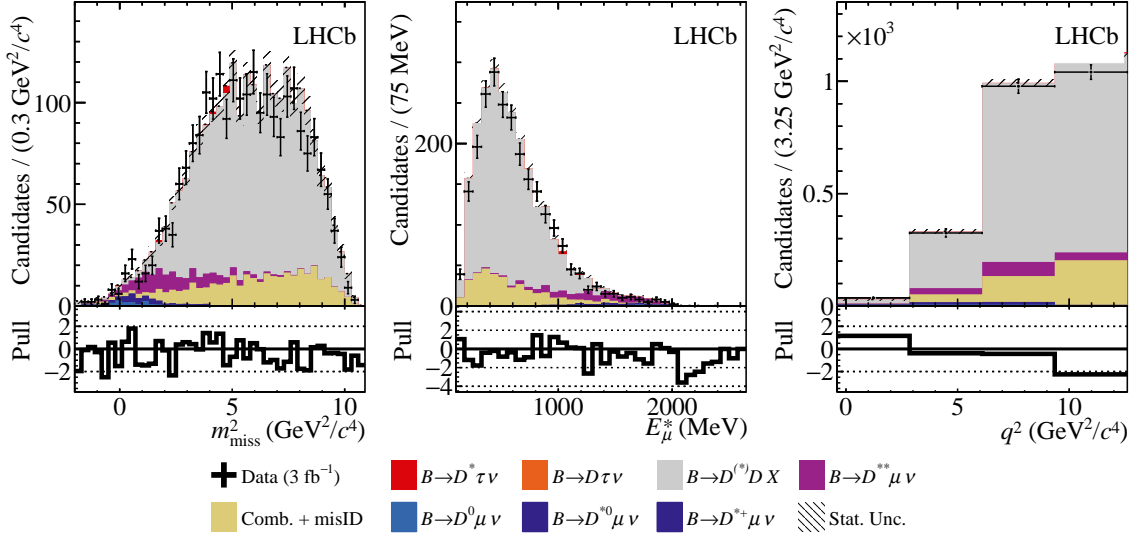


Figure 21: Distributions of (left) missing mass squared, (middle) lepton energy, and (right)  $q^2$ , overlaid with the projections of the fit model in the  $D^0\mu^-$  region with two opposite-sign kaons consistent with the  $B$  vertex, with a mass close to the nominal  $\phi$  mass. The label “stat. unc.” refers to the statistical uncertainty on the fitted sum of templates.

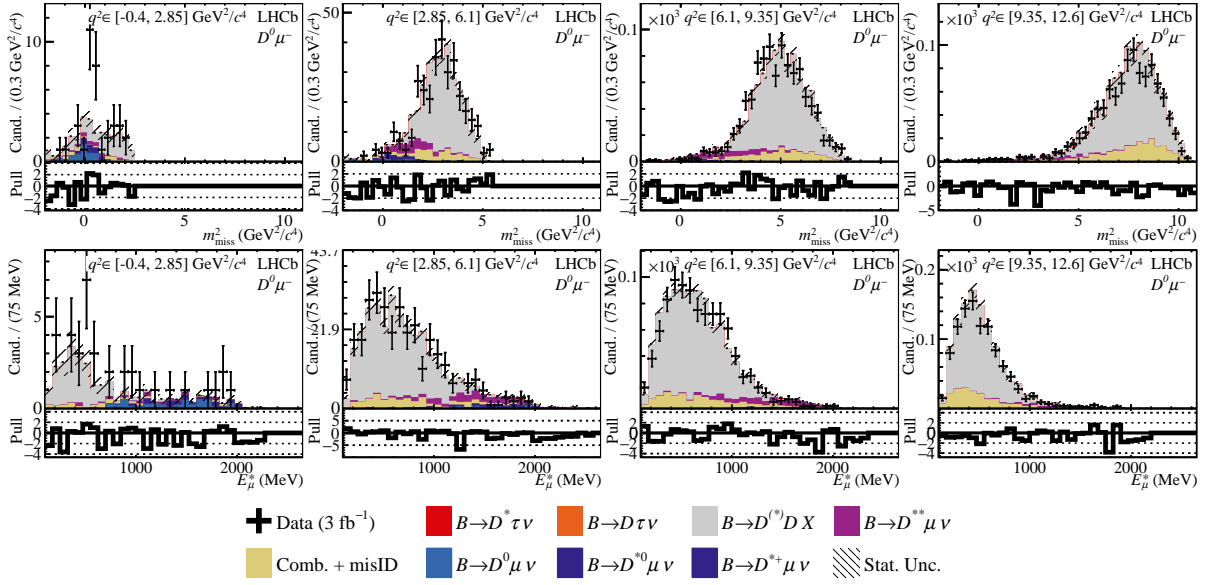


Figure 22: Distributions of (top row) missing mass squared and (bottom row) lepton energy overlaid with the projections of the fit model in the  $D^0\mu^-$  region with two opposite-sign kaons consistent with the  $B$  vertex, with a mass close to the nominal  $\phi$  mass, in the four bins of  $q^2$ . The label “stat. unc.” refers to the statistical uncertainty on the fitted sum of templates.

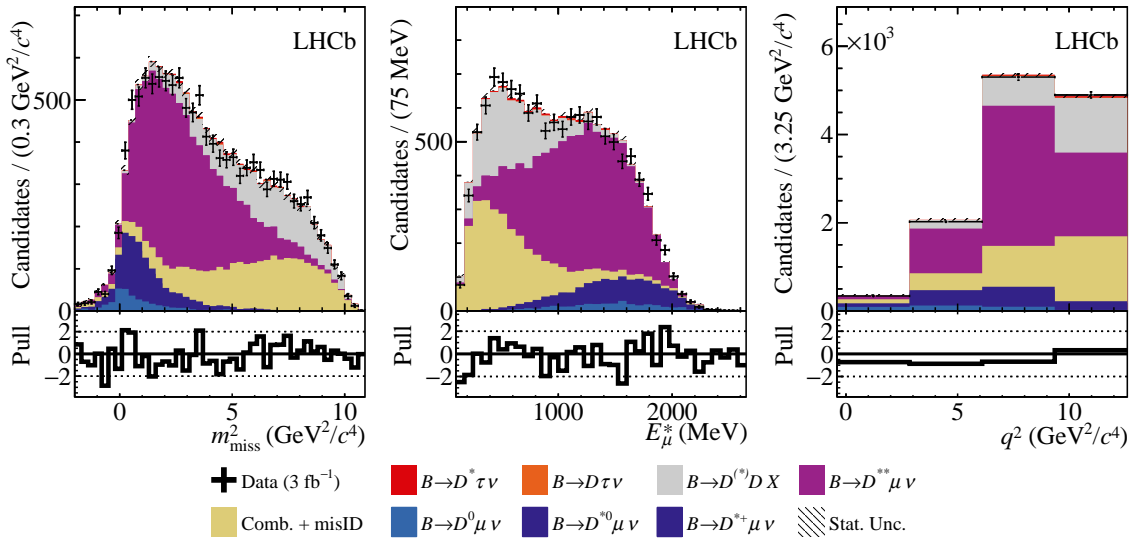


Figure 23: Distributions of (left) missing mass squared, (middle) lepton energy, and (right)  $q^2$ , overlaid with the projections of the fit model in the  $D^0\mu^-$  region with exactly two opposite-sign pions consistent with the  $B$  vertex, with a mass consistent with  $\eta \rightarrow \pi^+\pi^-\pi^0$  decays. The label “stat. unc.” refers to the statistical uncertainty on the fitted sum of templates.

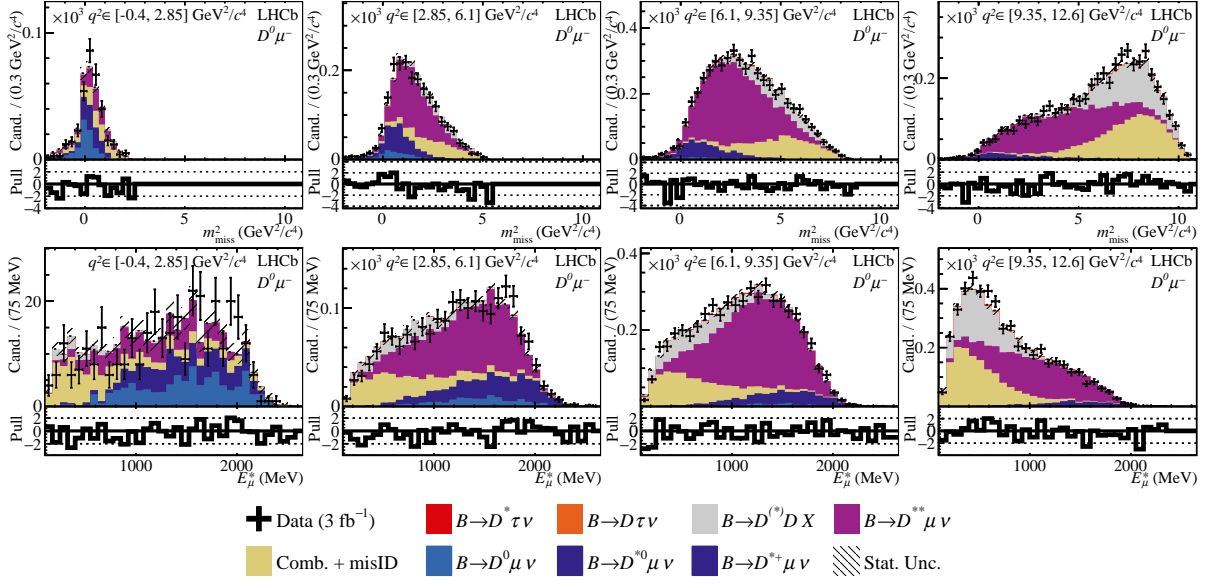


Figure 24: Distributions of (top row) missing mass squared and (bottom row) lepton energy overlaid with the projections of the fit model in the  $D^0\mu^-$  region with exactly two opposite-sign pions consistent with the  $B$  vertex, with a mass consistent with  $\eta \rightarrow \pi^+\pi^-\pi^0$  decays, in the four bins of  $q^2$ . The label “stat. unc.” refers to the statistical uncertainty on the fitted sum of templates.

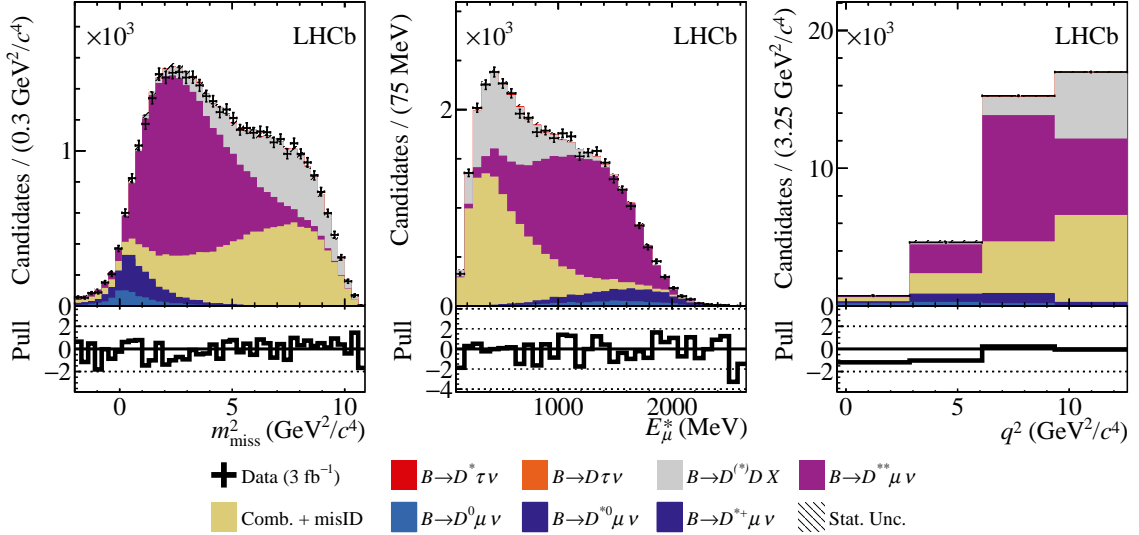


Figure 25: Distributions of (left) missing mass squared, (middle) lepton energy, and (right)  $q^2$ , overlaid with the projections of the fit model in the  $D^0\mu^-$  region with exactly two opposite-sign pions consistent with the  $B$  vertex, with a mass not consistent with  $\eta \rightarrow \pi^+\pi^-\pi^0$  decays. The label “stat. unc.” refers to the statistical uncertainty on the fitted sum of templates.

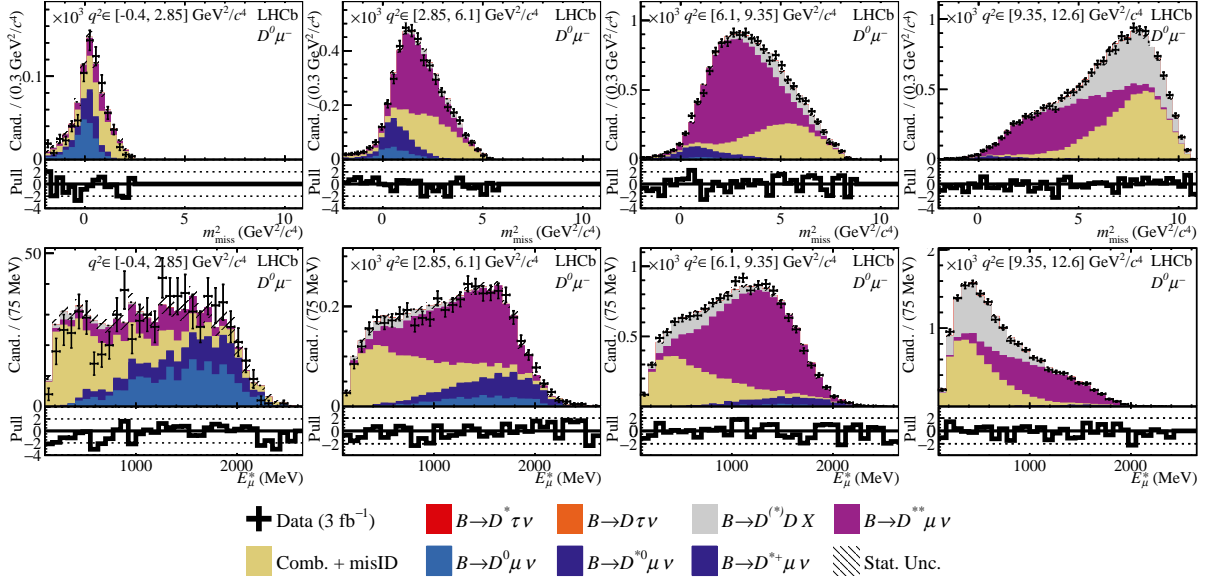


Figure 26: Distributions of (top row) missing mass squared and (bottom row) lepton energy overlaid with the projections of the fit model in the  $D^0\mu^-$  region with exactly two opposite-sign pions consistent with the  $B$  vertex, with a mass not consistent with  $\eta \rightarrow \pi^+\pi^-\pi^0$  decays, in the four bins of  $q^2$ . The label “stat. unc.” refers to the statistical uncertainty on the fitted sum of templates.

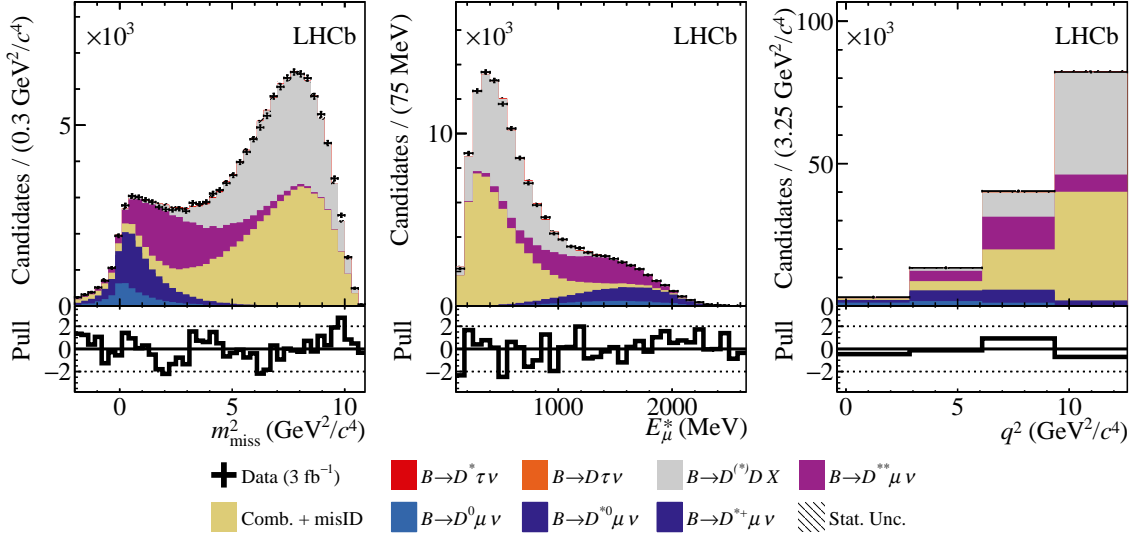


Figure 27: Distributions of (left) missing mass squared, (middle) lepton energy, and (right)  $q^2$ , overlaid with the projections of the fit model in the  $D^0\mu^-$  region with three pions consistent with the  $B$  vertex. The label “stat. unc.” refers to the statistical uncertainty on the fitted sum of templates.

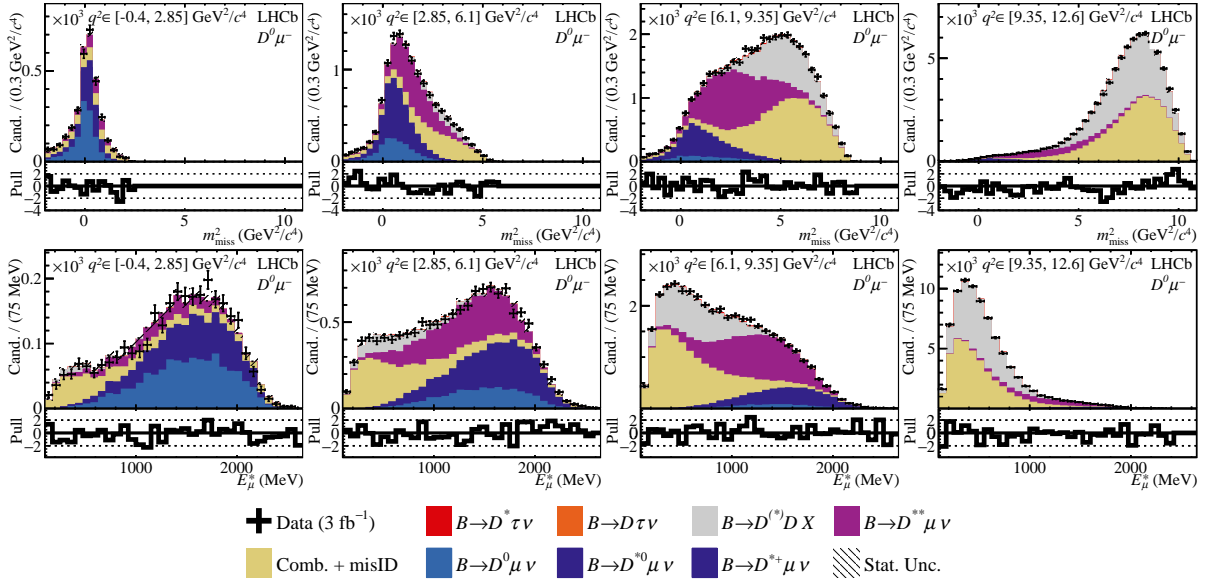


Figure 28: Distributions of (top row) missing mass squared and (bottom row) lepton energy overlaid with the projections of the fit model in the  $D^0 \mu^-$  region with three pions consistent with the  $B$  vertex, in the four bins of  $q^2$ . The label “stat. unc.” refers to the statistical uncertainty on the fitted sum of templates.

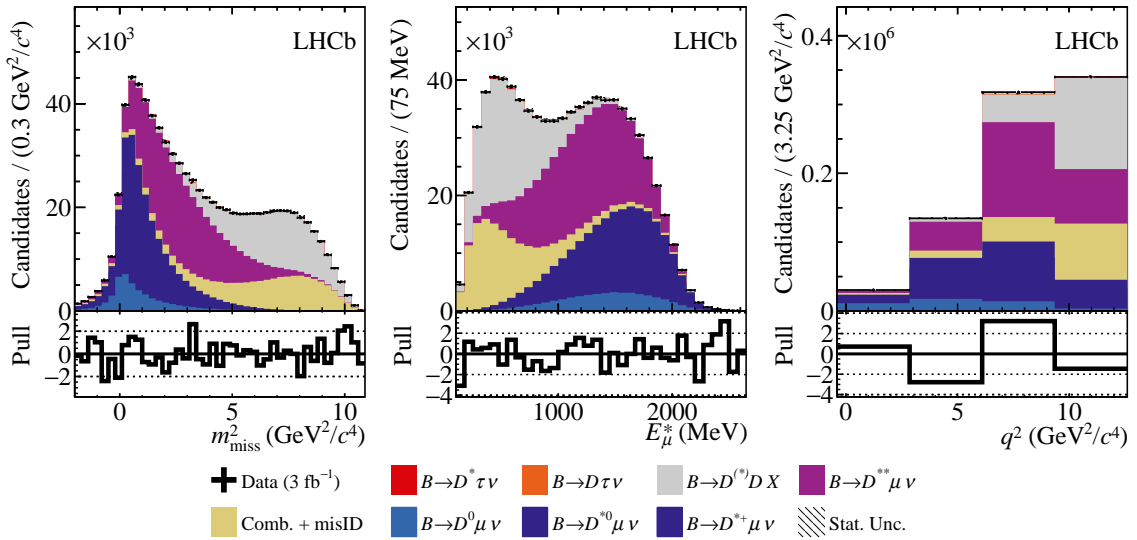


Figure 29: Distributions of (left) missing mass squared, (middle) lepton energy, and (right)  $q^2$ , overlaid with the projections of the fit model in the  $D^0 \mu^-$  region with any extra particle consistent with the  $B$  vertex. The label “stat. unc.” refers to the statistical uncertainty on the fitted sum of templates.



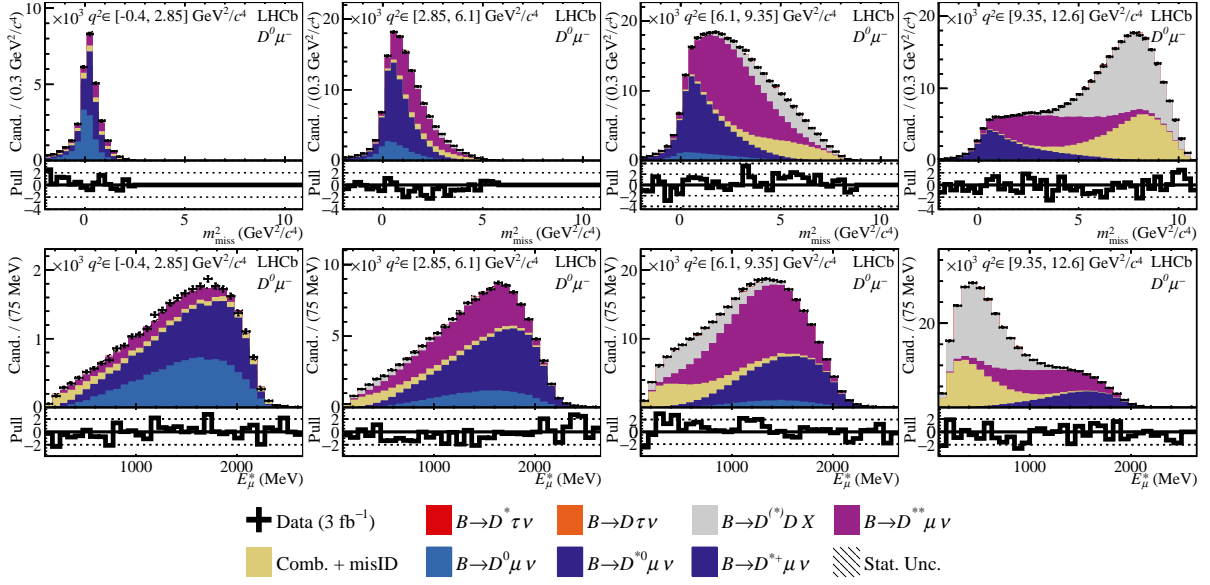


Figure 30: Distributions of (top row) missing mass squared and (bottom row) lepton energy overlaid with the projections of the fit model in the  $D^0\mu^-$  region with any extra particle consistent with the  $B$  vertex, in the four bins of  $q^2$ . The label “stat. unc.” refers to the statistical uncertainty on the fitted sum of templates.

### 1.3 Data - simulation comparison plots

In this section distributions are show for the following quantities: IP is defined as the distance of closest approach between a given particle trajectory and any primary vertex in the event;  $\chi_{\text{IP}}^2$  is defined as the difference in  $\chi^2/\text{ndof}$  for the primary vertex reconstructed with and without this particle trajectory included; DIRA is defined as the angle between the particle momentum direction and the line connecting the primary and decay vertices.

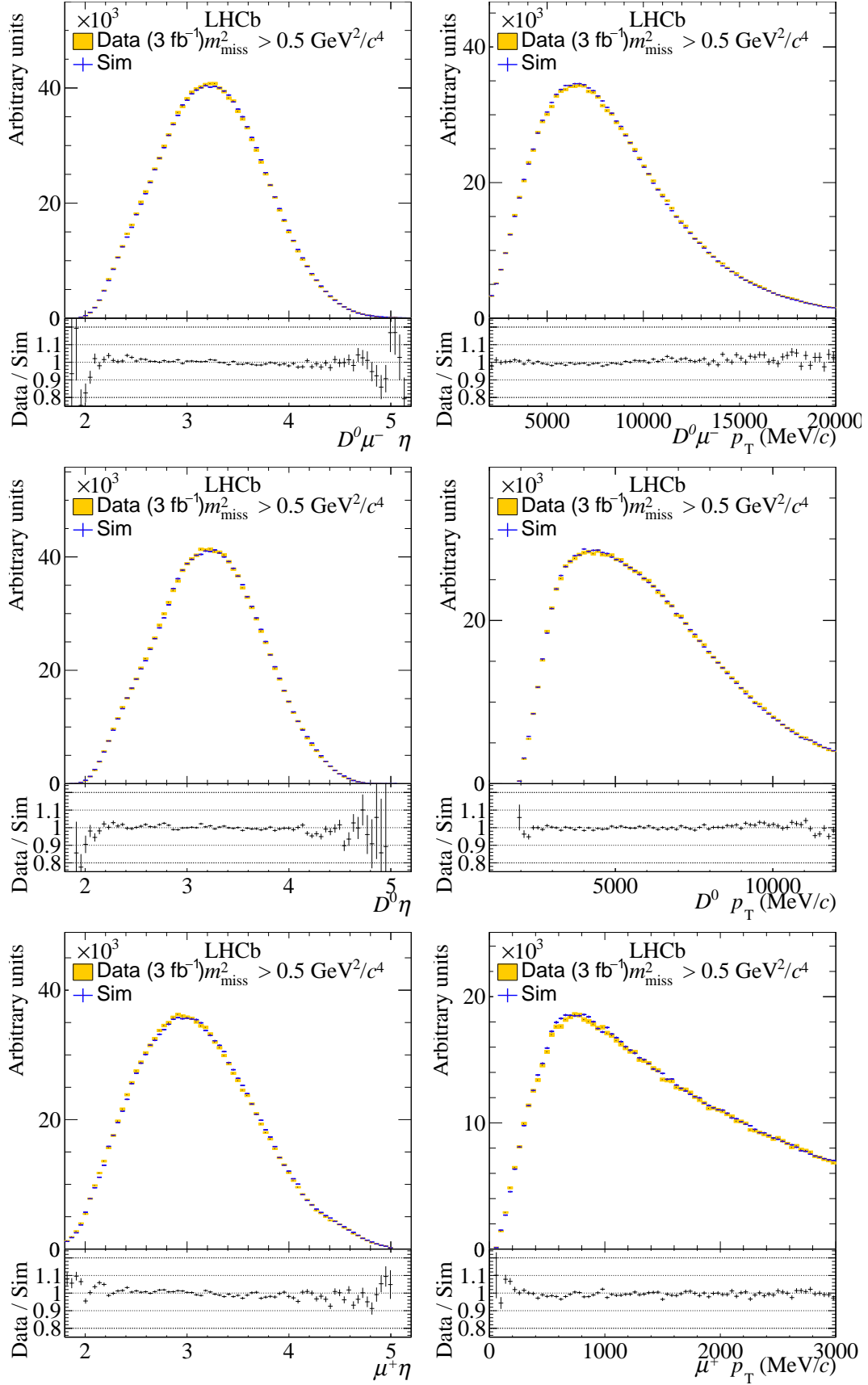


Figure 31: Distributions of kinematic variables in simulation and  $D^0\mu^-$  data, with the nominal corrections applied. The data correspond to the region with  $m_{\text{miss}}^2 > 0.5 \text{ GeV}^2/c^4$ , which is not used to generate corrections.

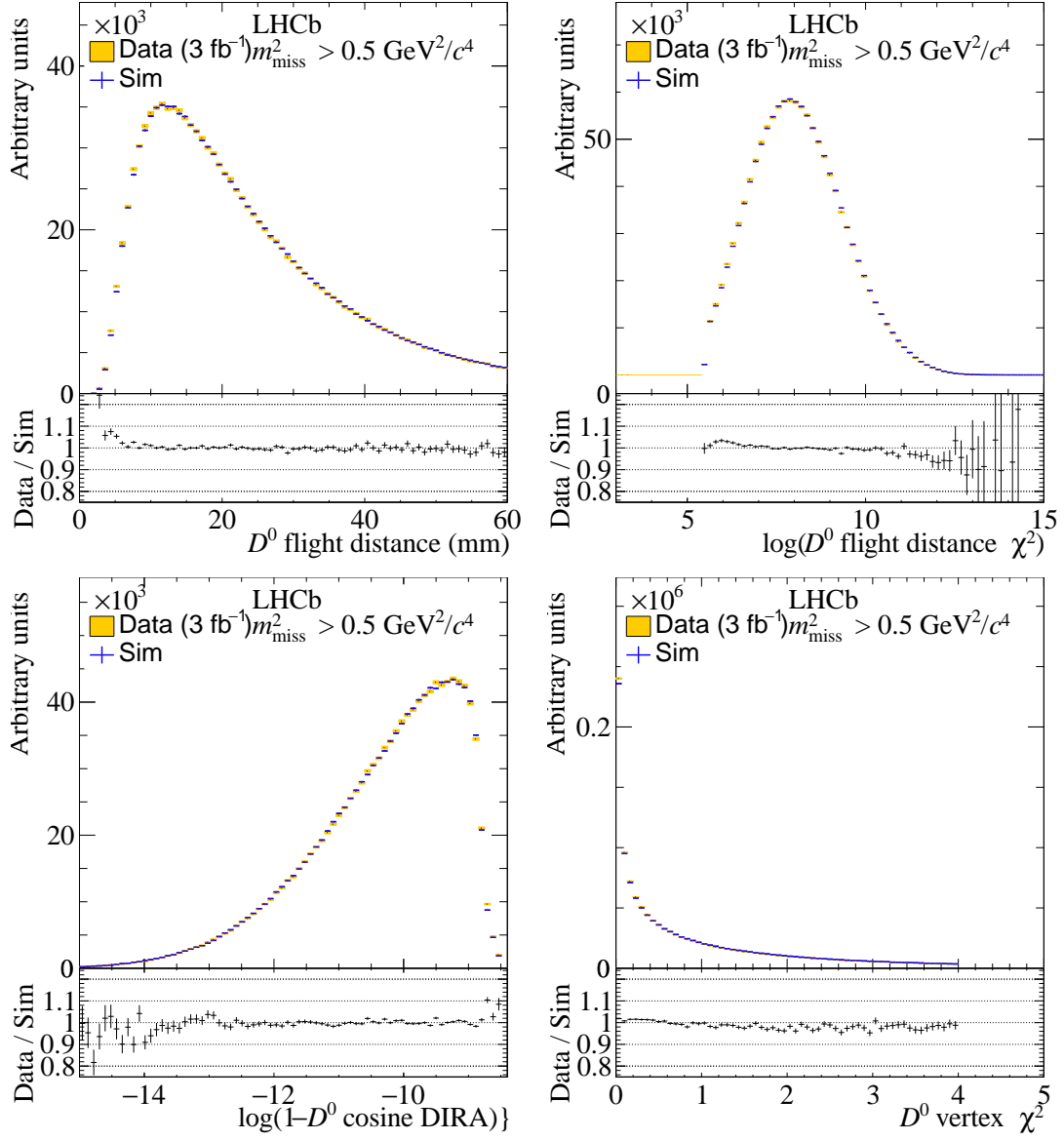


Figure 32: Distributions of geometric variables for  $D^0$  mesons in simulation and  $D^0\mu^-$  data, with the nominal corrections applied. The data correspond to the region with  $m_{\text{miss}}^2 > 0.5 \text{ GeV}^2/c^4$ , which is not used to generate corrections.

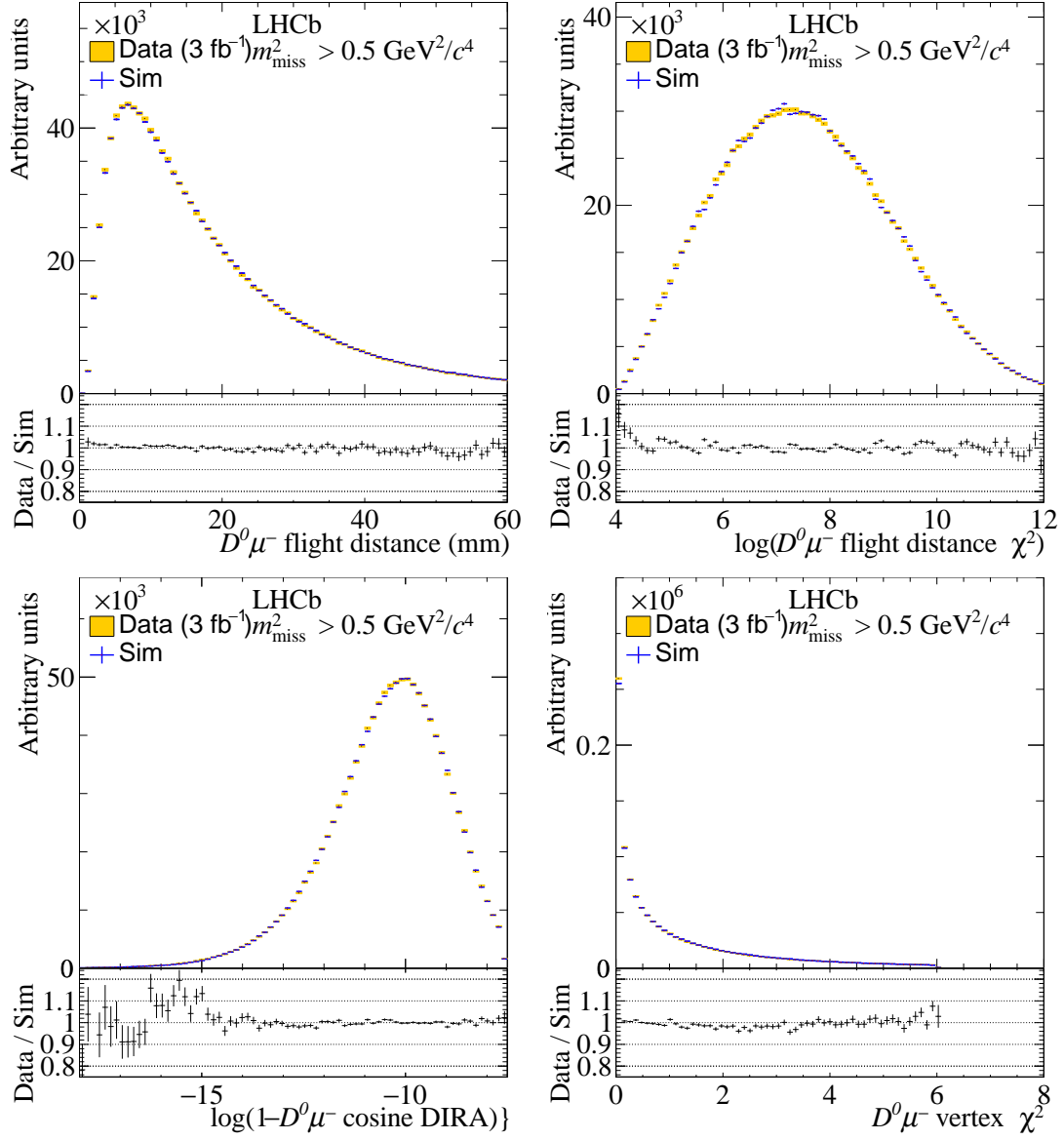


Figure 33: Distributions of geometric variables in simulation and  $D^0\mu^-$  data, with the nominal corrections applied. The data correspond to the region with  $m_{\text{miss}}^2 > 0.5 \text{ GeV}^2/c^4$ , which is not used to generate corrections.

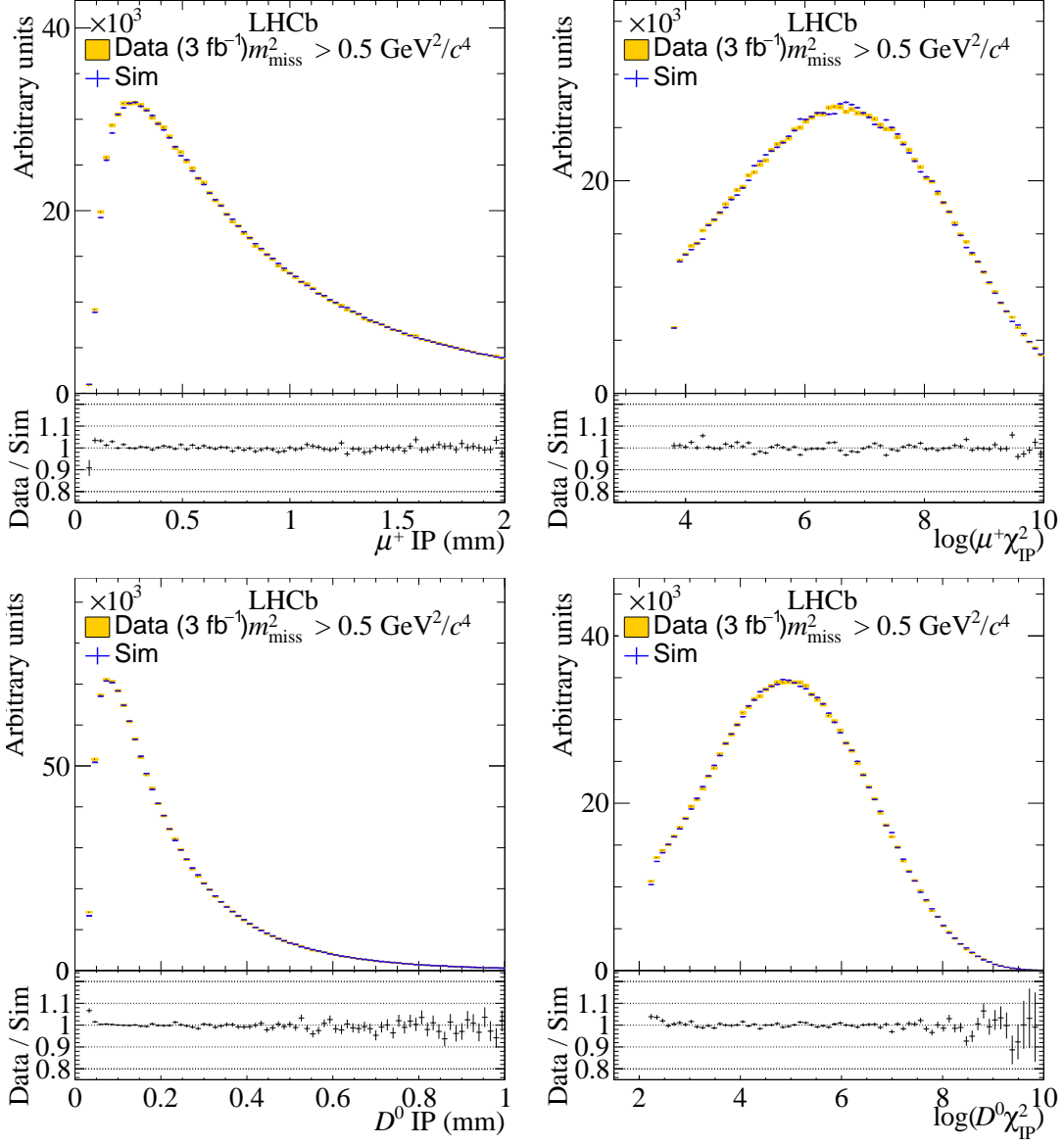


Figure 34: Distributions of impact parameter and the quantity  $\chi_{\text{IP}}^2$  in simulation and  $D^0\mu^-$  data, with the nominal corrections applied. The data correspond to the region with  $m_{\text{miss}}^2 > 0.5 \text{ GeV}^2/c^4$ , which is not used to generate corrections.

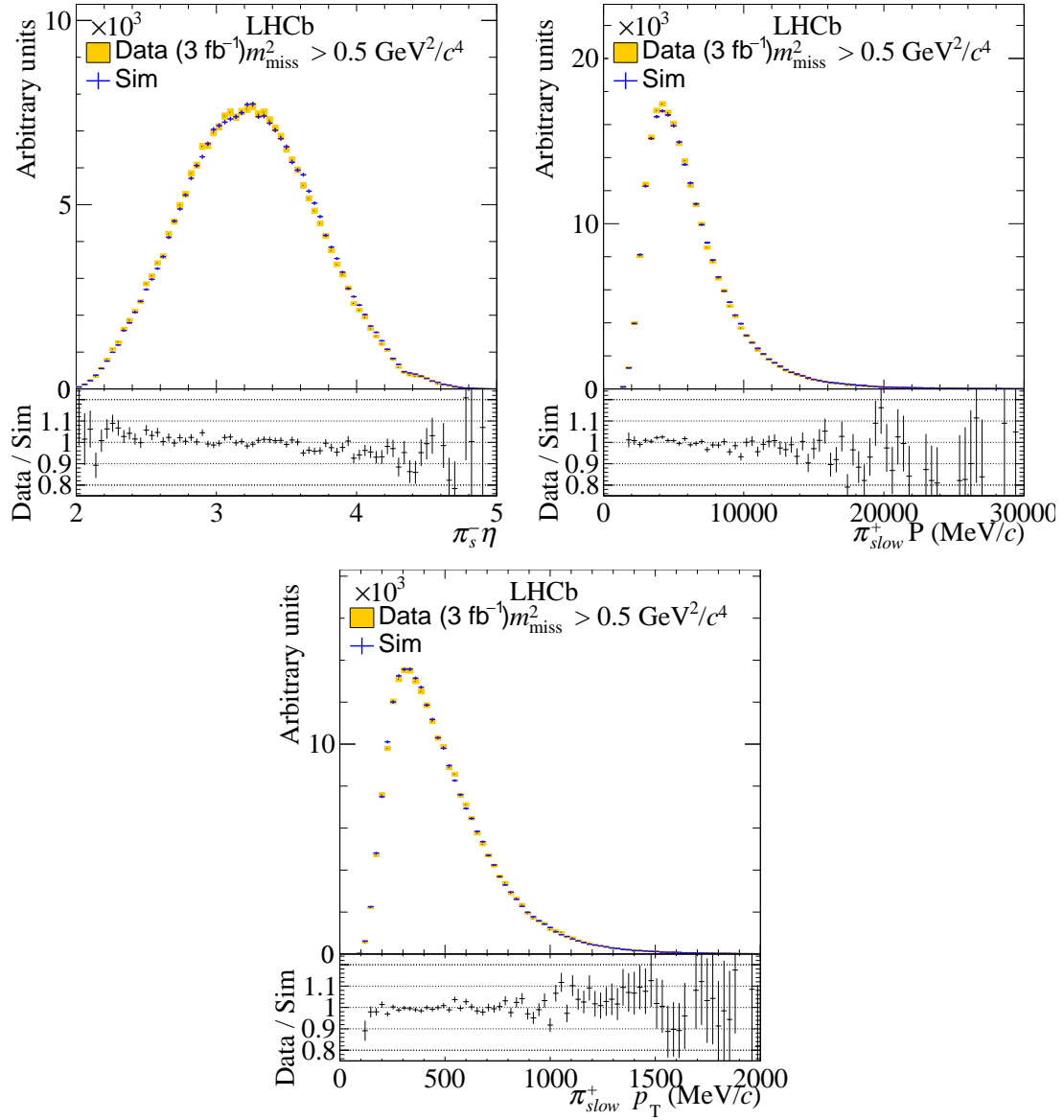


Figure 35: Distributions of kinematic variables in simulation and  $D^{*+}\mu^-$  data, with the nominal corrections applied. The data correspond to the region with  $m_{\text{miss}}^2 > 0.5 \text{ GeV}^2/c^4$ , which is not used to generate corrections.

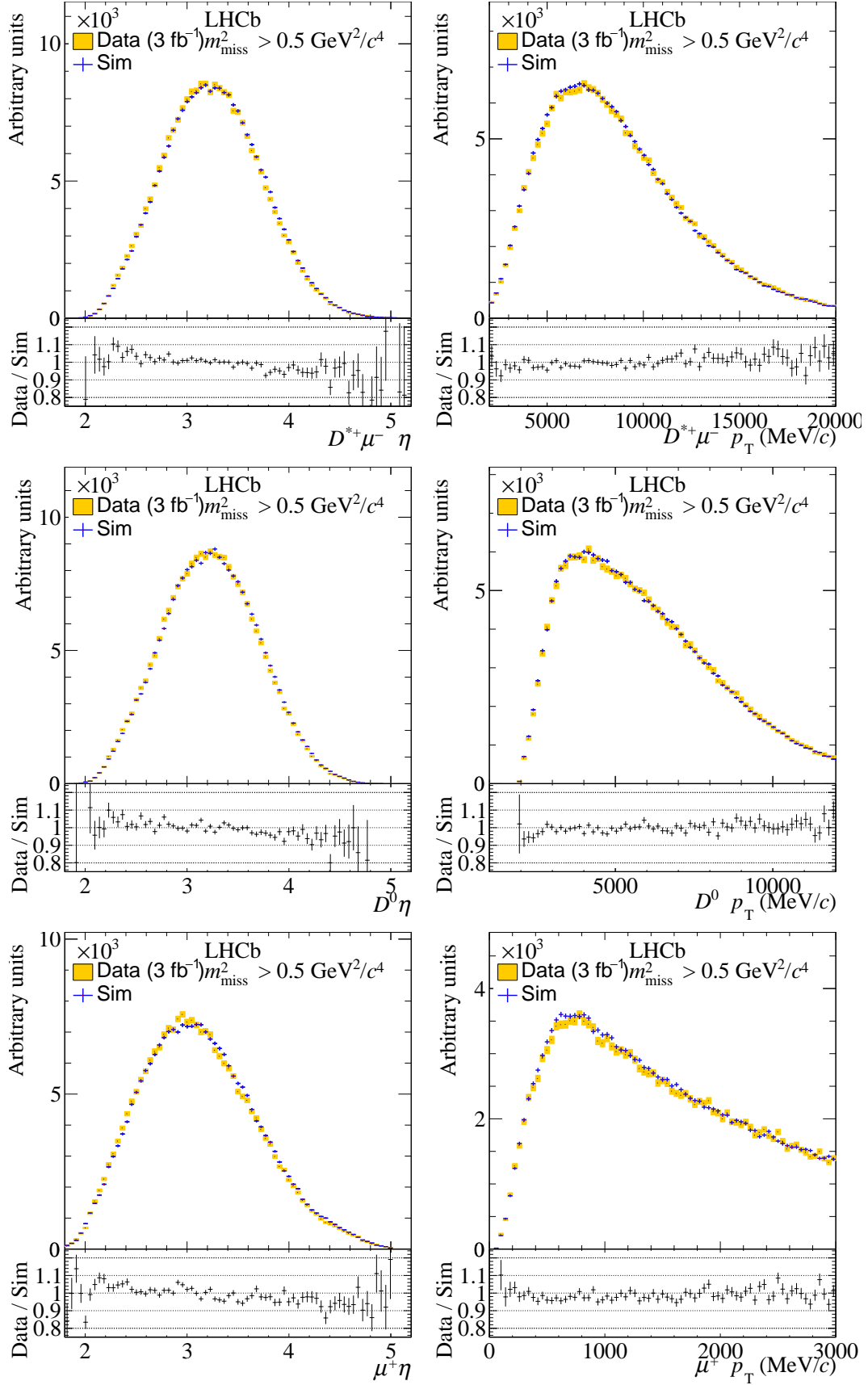


Figure 36: Distributions of kinematic variables in simulation and  $D^{*+}\mu^-$  data, with the nominal corrections applied. The data correspond to the region with  $m_{\text{miss}}^2 > 0.5 \text{ GeV}^2/c^4$ , which is not used to generate corrections.

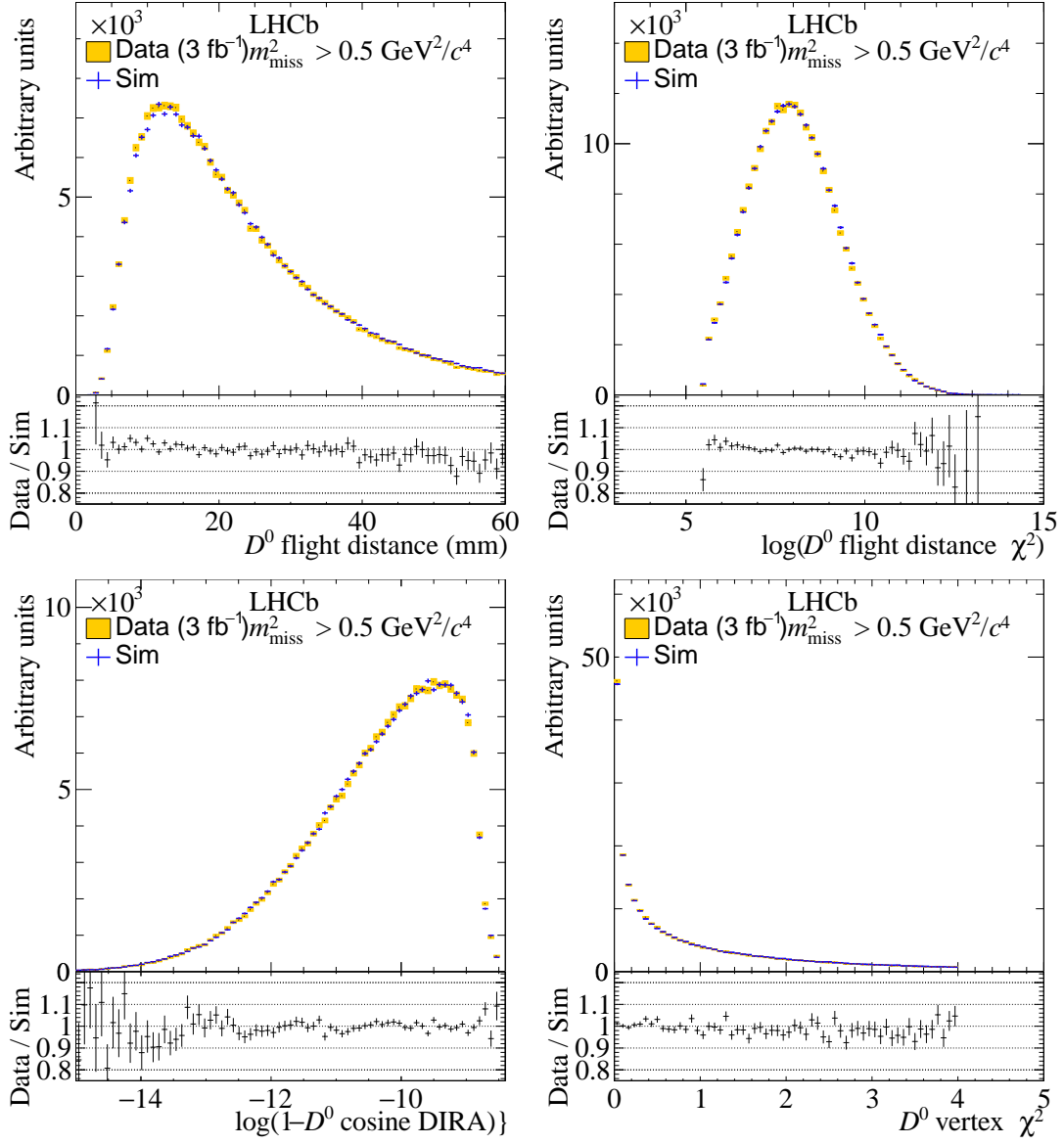


Figure 37: Distributions of geometric variables for  $D^0$  mesons in simulation and  $D^{*+}\mu^-$  data, with the nominal corrections applied. The data correspond to the region with  $m_{\text{miss}}^2 > 0.5 \text{ GeV}^2/c^4$ , which is not used to generate corrections.



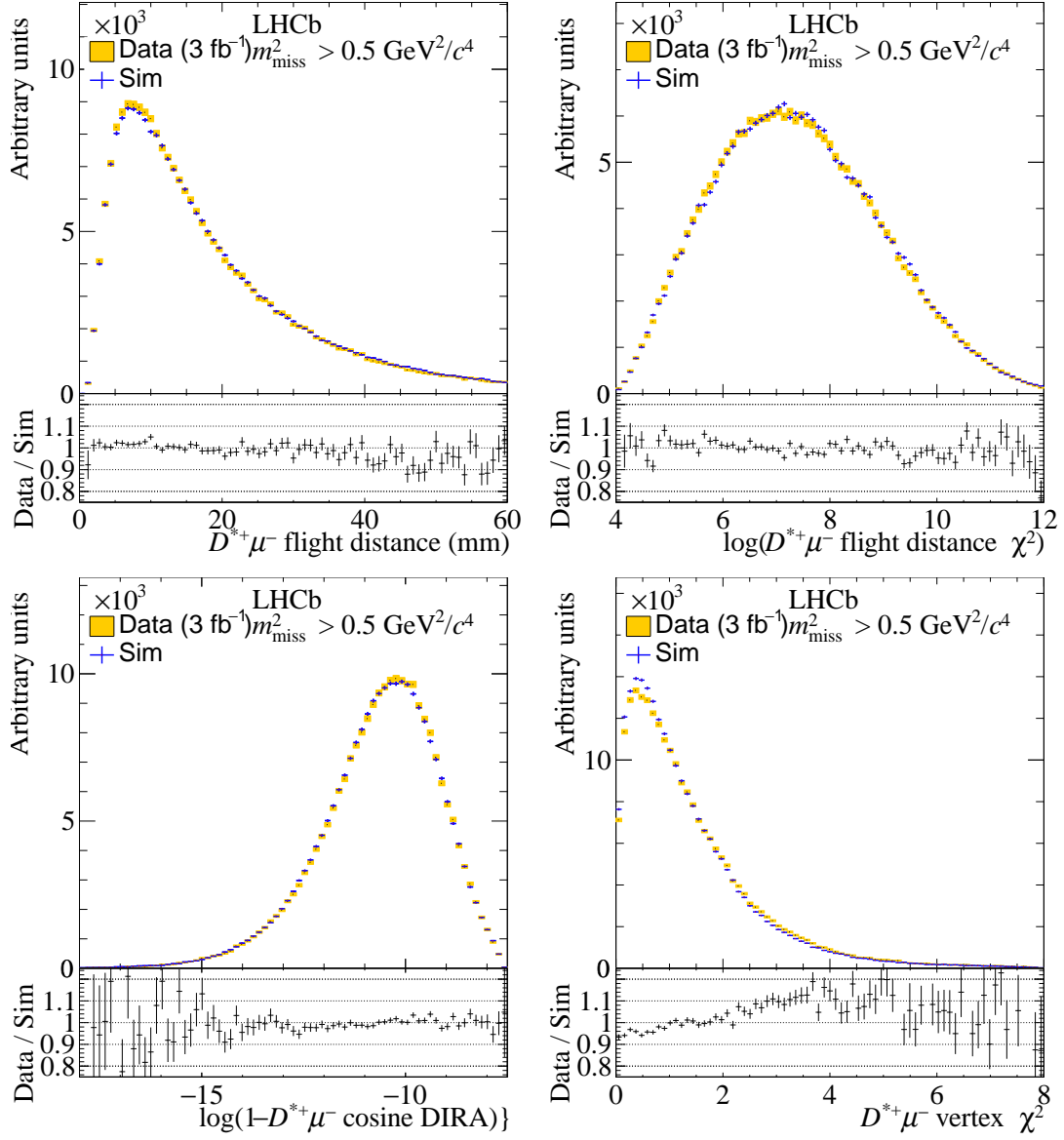


Figure 38: Distributions of geometric variables in simulation and  $D^{*+}\mu^-$  data, with the nominal corrections applied. The data correspond to the region with  $m_{\text{miss}}^2 > 0.5 \text{ GeV}^2/c^4$ , which is not used to generate corrections.

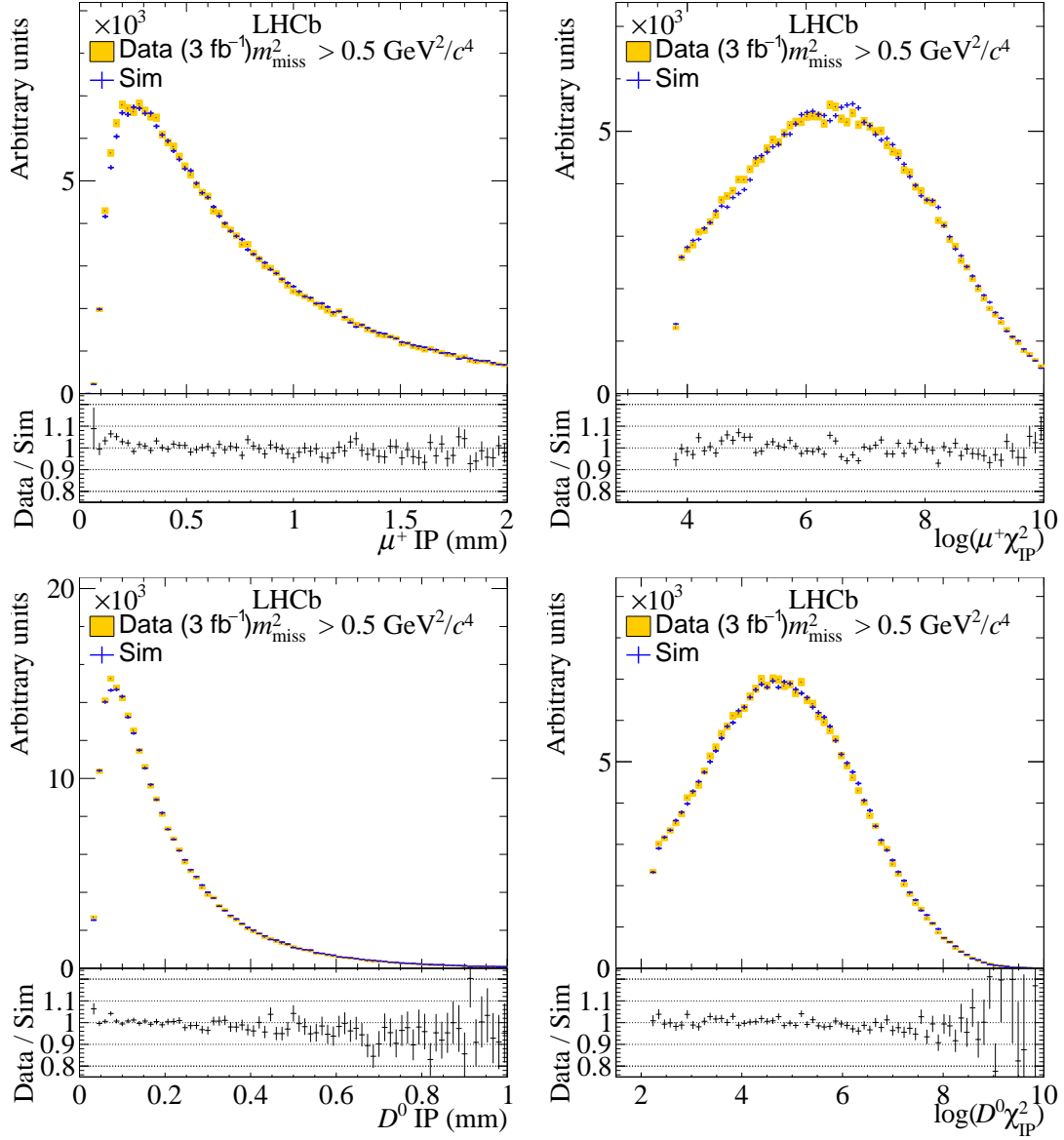


Figure 39: Distributions of impact parameter and the quantity  $\chi_{\text{IP}}^2$  in simulation and  $D^{*+}\mu^-$  data, with the nominal corrections applied. The data correspond to the region with  $m_{\text{miss}}^2 > 0.5 \text{ GeV}^2/c^4$ , which is not used to generate corrections.

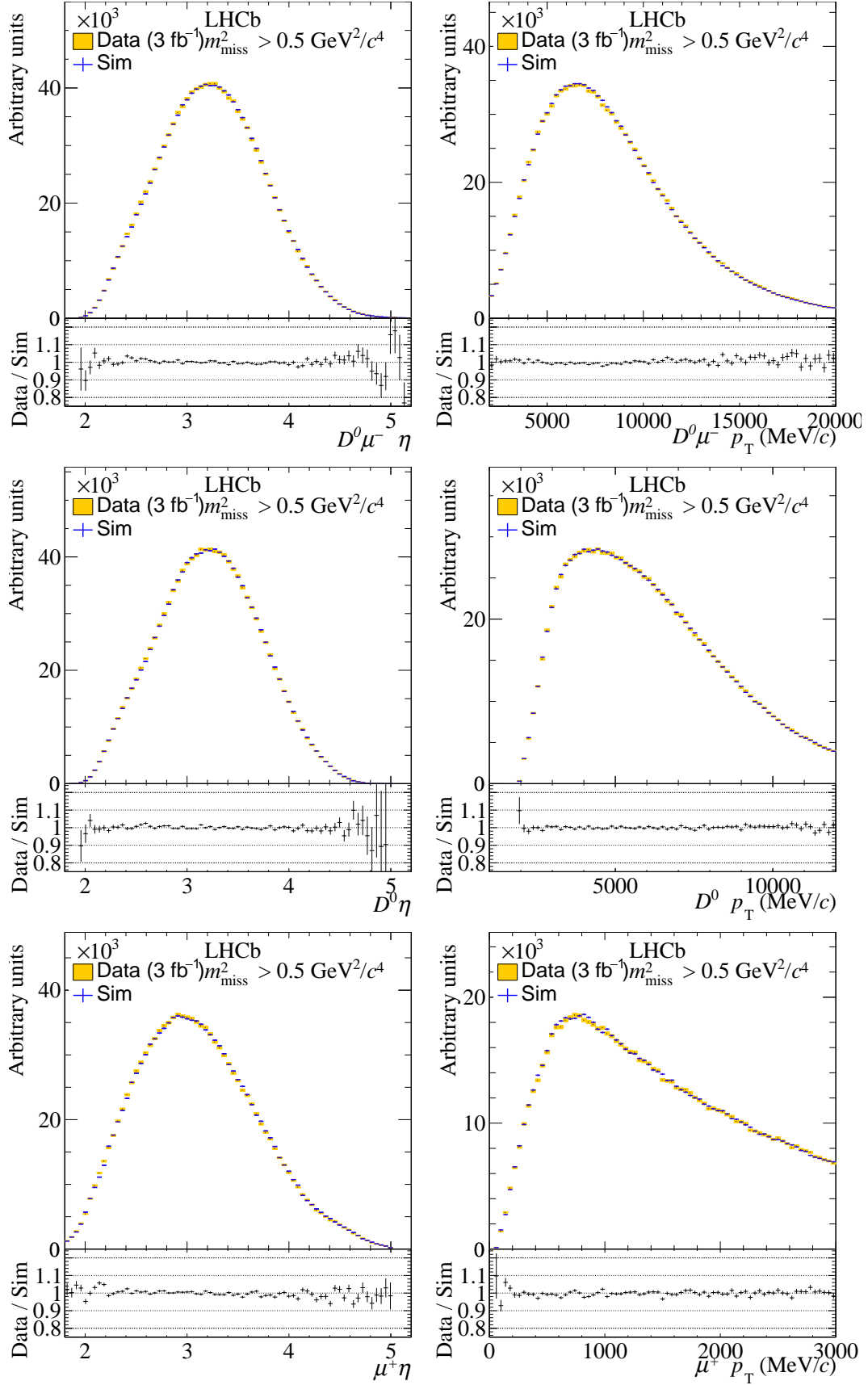


Figure 40: Distributions of kinematic variables in simulation and  $D^0 \mu^-$  data, with the second iteration of the corrections applied. The data correspond to the region with  $m_{\text{miss}}^2 > 0.5 \text{ GeV}^2/c^4$ , which is not used to generate corrections.

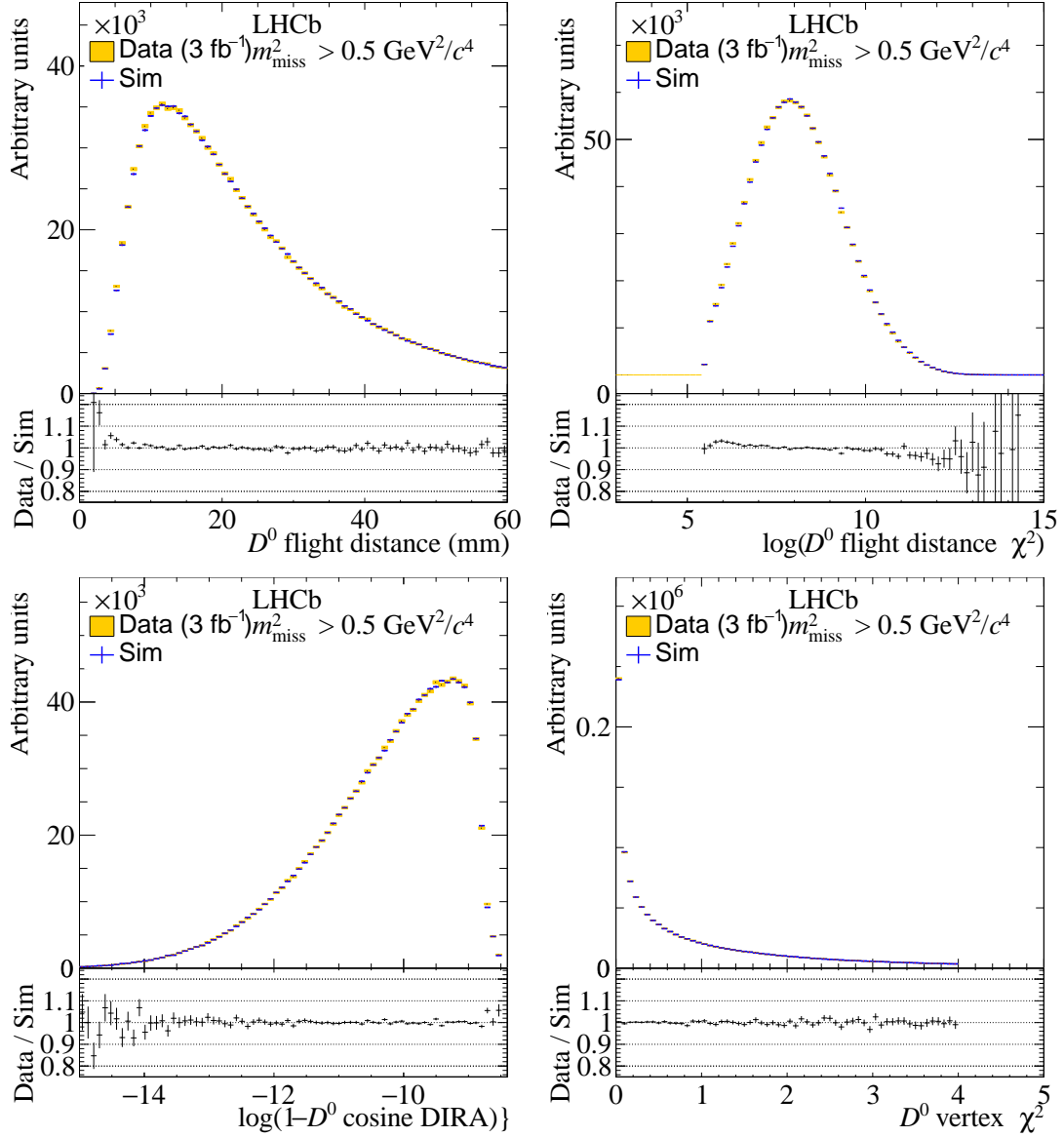


Figure 41: Distributions of geometric variables for  $D^0$  mesons in simulation and  $D^0\mu^-$  data, with the second iteration of the corrections applied. The data correspond to the region with  $m_{\text{miss}}^2 > 0.5 \text{ GeV}^2/c^4$ , which is not used to generate corrections.

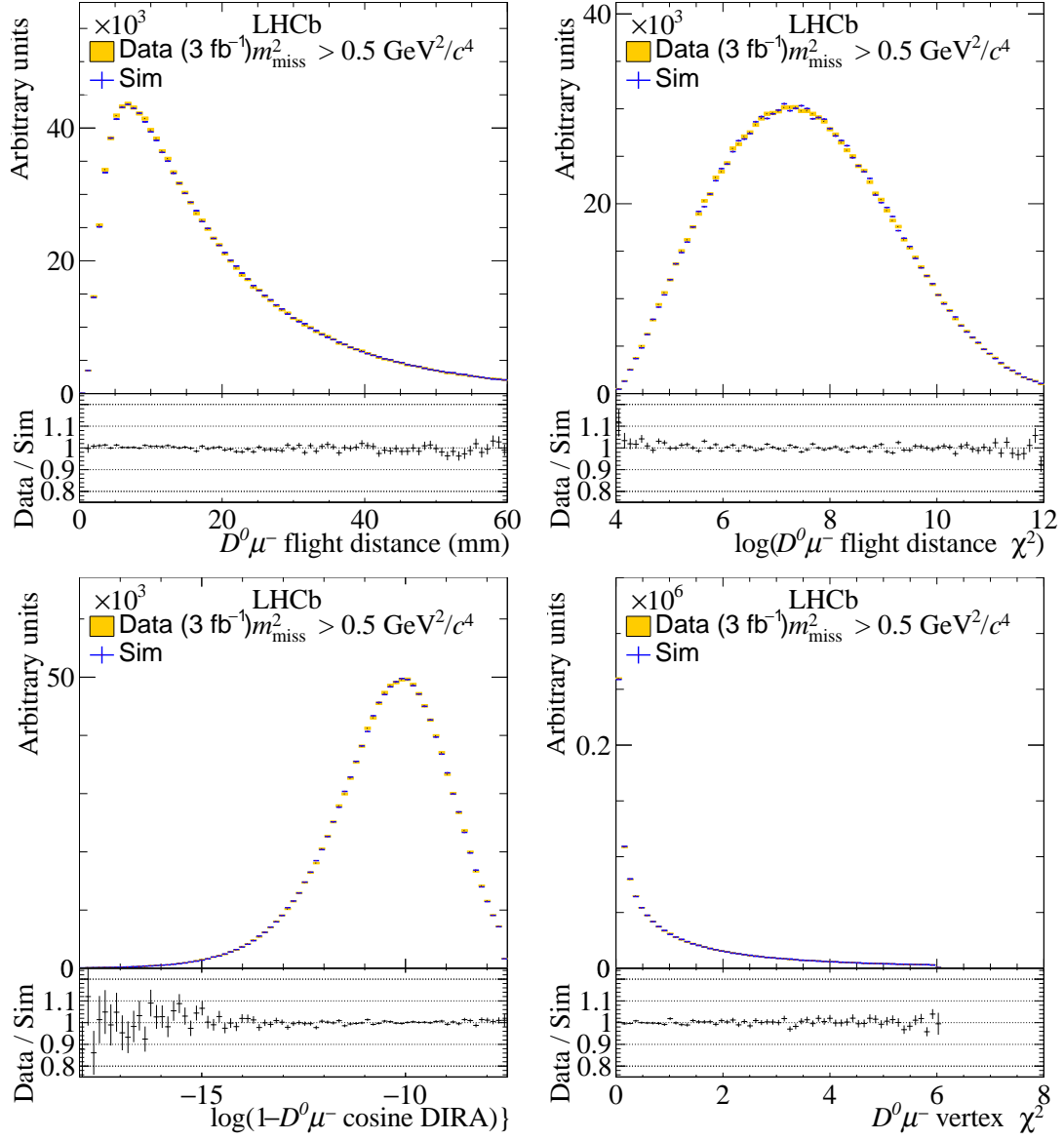


Figure 42: Distributions of geometric variables in simulation and  $D^0\mu^-$  data, with the second iteration of the corrections applied. The data correspond to the region with  $m_{\text{miss}}^2 > 0.5 \text{ GeV}^2/c^4$ , which is not used to generate corrections.

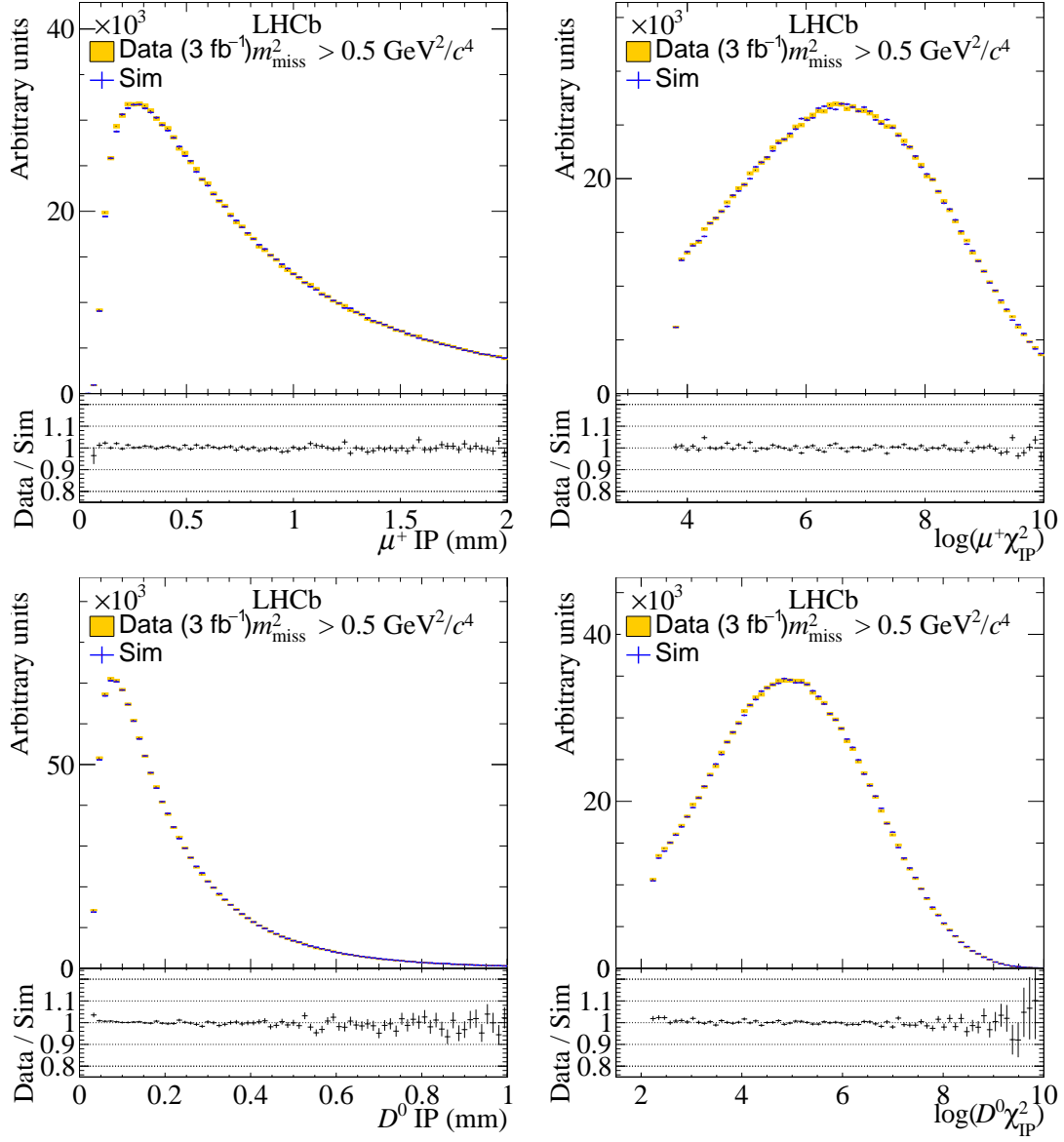


Figure 43: Distributions of impact parameter and the quantity  $\chi_{\text{IP}}^2$  in simulation and  $D^0 \mu^-$  data, with the second iteration of the corrections applied. The data correspond to the region with  $m_{\text{miss}}^2 > 0.5 \text{ GeV}^2/c^4$ , which is not used to generate corrections.